Journal of Ship Production and Design, Vol. 37, No. 3, August 2021, pp. 159–180
http://dx.doi.org/10.5957/JSPD.11180039

A Review of Hydrodynamic Design Methods for Seaplanes

Michael G. Morabito

Department of Naval Architecture and Ocean Engineering, United States Naval Academy, Annapolis, Maryland

The design of successful water-based aircraft requires a close collaboration between the aeronautical engineers and naval architects, who perform high-speed towing tests, stability calculations, or computational fluid dynamics in support of the design. This article presents the fundamental design considerations of waterborne aircraft, which are outside of the typical educational scope of most naval architects, but which they are sometimes asked to address. These include 1) the hydrostatic and hydrodynamic problems associated with seaplane design, 2) early-stage methods for sizing the hull, 3) prediction techniques using archival data, and 4) hydrodynamic model testing procedures. Although a new design will often require substantial iteration to achieve the desired outcome, the information in this article will assist in developing a reasonable starting point for the design spiral and provides sufficient details for a hydrodynamic model testing facility to perform a successful series of model tests on the design. Although much of the work in this field dates from the 1940s, it is important to review this material in light of the current practices being used at hydrodynamic research facilities today. A detailed description of the model testing apparatus and procedure, used in a recent study at the U.S. Naval Academy, is presented to demonstrate the current applicability of these methods and some pitfalls that can be expected in testing.

Keywords: seaplane; flying boat; planing; towing tank; high-speed

1. Introduction

Today, there is a renewed interest in seaplane designs for both civilian and governmental applications worldwide. According to the Seaplane Pilots Association, there are approximately thirty-five thousand seaplane-rated pilots in the United States and between five and ten thousand operational seaplanes. Worldwide, larger seaplanes are used for firefighting, search and rescue applications, and cargo transportation.

Although seaplane design work in the United States is less abundant now than it was in the post-WWII era, the high-speed towing tanks at the U.S. Naval Academy, Stevens Institute of Technology, and David Taylor Model Basin have all underwent some form of seaplane towing tests within the last 5 years. This article provides fundamental information that is useful both to designers and to those conducting physical model testing. Although the design is ordinarily led by those in the aerospace industry, naval architects with experience in high-speed planing craft are often brought in to a seaplane project to provide insights into the following areas:

1) preparation of hydrostatic stability calculations,
2) performance predictions using archival data,
3) towing tank or CFD predictions, and
4) Diagnosing problems with takeoff and landing of existing seaplanes.

2. Current interest in seaplanes

Most seaplanes manufactured today are small "floatplanes," which are stock aircraft fitted with stock floats from a variety of manufacturers. The floats are designed to meet standards for stability, reserve buoyancy, compartmentalization, and structural design (see Code of Federal Regulations (CFR) Title 14: Parts 23 and 25). Successful floatplanes are airplanes with low takeoff speed, to reduce landing impact accelerations, and high bollard pull thrust, to overcome hydrodynamic resistance.

Some emerging seaplane missions include a new class of light recreational aircraft permitted by the Federal Aviation Administration,

Manuscript received by JSPD Committee April 28, 2020; accepted December 14, 2020.

Corresponding author: Michael G. Morabito, morabito@usna.edu

typified by the Icon A5 (Fig. 1), and small, unmanned seaplanes. In 2006, Oregon Iron Works successfully conducted the first autolanding of an unmanned seaplane in the United States. Today, unmanned seaplanes are currently in production (Fig. 2).

There are a small number of manufacturers of larger "flying boats," which are purpose-built seaplanes in which the hydrodynamic hull is built into the bottom of the fuselage; e.g., Bombardier (Canada) has produced more than 80 large firefighting seaplanes since the early 1990s. Beriev Aircraft Company (Russia) produces the Be-200 multipurpose amphibious craft, which can perform search and rescue, aerial firefighting, cargo transport, and passenger service. With a maximum takeoff weight of 37 tons and a wingspan of 33 m, it is one of the largest production seaplanes. Today, the Aviation Industry Corporation of China is testing a prototype TA600, a 50-ton, 40-m wingspan flying boat capable of aerial firefighting and search and rescue operations (Fig. 3). It is slightly larger than a Boeing 737.

Within the last decade, there has been government interest in seaplane operations as well. In the United States, Carderock's Center for Innovation in Ship Design studied the potential use of seaplanes within a seabasing environment (Odedra et al. 2004; Denz et al. 2007). The U.S. Naval Air Warfare Center studied the potential effect of maturing technology on future seaplane designs (Bellanca & Matthews 2005). NASA has recently been reviewing classification of civil unmanned aircraft, including seaplanes (Hayhurst et al. 2014). FUSETRA, a European Union–supported project, produced a series of reports focusing on development of future seaplane transportation. Partner institutions included the University of Glasgow, Dornier Aviation, Rzeszow University, and TU Munich (Gobbi et al. 2011; Majka et al. 2011; Mohr et al. 2011).

There has been a growth in academic research, conference papers, and journal articles. The University of Glasgow has had a series of master's theses in seaplane design. Ying-gu et al. (2011) of the Chinese Academy of Sciences modeled the longitudinal aerodynamic and hydrodynamic effects of a flying boat in calm water, using a modification of the Savitsky (1964) method. Nebylov and Nebylov (2011) of St. Petersburg studied optimizing landing wave heading for reduced impact accelerations. Du et al. (2014), of China, studied autonomous takeoff control systems for unmanned seaplanes. Dala (2015), of South Africa, studied porpoising stability

Fig. 1 Icon A5 seaplane (taken from CNN.com)

in a circulating water channel. With new designs of large flying boats coming out, large numbers of recreational, commercial, and governmental seaplanes worldwide and a growing research presence, there is an increasing need for practical design information.

The coupled aerohydrodynamic problem of landing and takeoff of seaplanes is especially well suited to the application of computational fluid dynamics because of the inherent approximations that need to be made to tow a model at a Froude-scaled speed in a towing tank, when the aerodynamics are better served with Reynolds scaling. As the computational techniques continue to improve, researchers are now capable of handling some of the most difficult problems. Feng et al. (2020) studied the problem of seaplane landing impact in waves using computational fluid dynamics. Duan et al. (2019) investigated the porpoising motion of a seaplane using a two-phase solver in OpenFOAM, simulating a large four-turbine seaplane, including the effects of ground effect and slipstream.

Although the computational methods are continuing to increase in ability, we have seen internationally that the towing tank has remained the centerpiece of seaplane hydrodynamic analysis worldwide. Xao et al. (2019) provide a computational study of the effects of blockage on the aviation high-speed towing tank in an article that features the impressive modern facilities that they are using for seaplane model testing.

Nomenclature

AR = aspect ratio = $\frac{\text{Span}^2}{\text{Wing Area}}$
B = beam (m)
b_w = wingspan (m)
c = distance from the center of the tip float to the centerline of the seaplane.
C_{DA} = aerodynamic drag coefficient
C_L = lift coefficient, $C_L = \frac{\Delta}{\frac{1}{2}\rho V^2 B^2}$
C_{LA} = aerodynamic lift coefficient, $C_{\text{LA}} = \frac{L_A}{\frac{1}{2}\rho_A V^2 S}$
C_{LAmax} = maximum aerodynamic lift coefficient
C_Δ = load coefficient, $C_\Delta = \frac{\Delta}{\rho g B^3}$
C_{Δ_O} = static load coefficient, $C_{\Delta_O} = \frac{\Delta_O}{\rho g B^3} = K_2 \left(\frac{L}{B}\right)^2$
D_A = aerodynamic drag (N)
e = planform efficiency factor
K_2 = Davidson static load coefficient, $K_2 = \frac{\Delta_O}{\rho g L^2 B}$
k = Parkinson forebody load coefficient, $k = \frac{\Delta_O}{\rho g L_f^2 B}$
$h_{\%b}$ = step height (% of beam)
h_e = absolute value of the negative metacentric height at zero heel (m)
$h_{1/3}$ = the significant wave height (m)
L_A = aerodynamic lift (N)
L_a = afterbody length (m)
L_f = forebody length (m)
L = length of float, from the bow to sternpost (m)
S = wing area (sq. m)
V = velocity (m/sec)
V_G = getaway, or takeoff speed (m/sec)
α = afterbody angle (deg)
β = deadrise angle (deg)
σ = sternpost angle (deg)
ϕ_1 = the heel angle required to submerge the float (deg)
ρ = mass density of water (kg/m^3)
ρ_A = mass density of air (kg/m^3)
η = impact acceleration (g's)
γ = the flight path angle (deg)
γ_e = effective flight path angle in rough water (deg)
Δ = weight on water, which varies with speed due to wing unloading (N)
Δ_O = static weight (N)
Δ_T = the fully immersed displacement of each tip float (N)

Fig. 2 China's U650 amphibious drone (taken from China Daily)

2.1. Focus of the present paper

This article provides the information necessary to use existing high-speed towing facilities and personnel to the task of seaplane hydrodynamic evaluation as the need arises. The following sections provide groundwork for understanding the design and hydrodynamic evaluation of seaplanes. This necessarily relies on a long history stretching back to before the Second World War. The article culminates with the design, fabrication, and testing of a new seaplane test apparatus at the U.S. Naval Academy, designed to perform 1) low-speed free-to-trim tests, 2) high-speed fixed-trim tests, and 3) dynamic stability tests. This towing fixture uses mechanical means to represent the aerodynamic forces of the wing and tail surfaces, which are not easily modeled in a Froude-scaled test. A case study is provided showing how the new test apparatus was used in the concept design phase to identify a porpoising instability early on and the methods used to correct it.

In the short time that this article has been under review, the Naval Academy has fabricated a second, larger, test apparatus on the same principles and conducted systematic model tests on the hydrodynamic lift, drag, and porpoising inception of cambered planing surfaces for stepped planing hulls with hydrofoil stabilizers. Model tests of a complete hydrofoil-stabilized stepped planing hull (Brizzolara et al. 2016) showed a dynamic instability in pitch and heave that was not easily explained. The new physical model tests, made on the seaplane apparatus, showed that the hull was dynamically stable, helping us identify the intermittent ventilation of the stern hydrofoil as the culprit. These tests also enabled a CFD validation study of the hull itself, the results of which should be available at the 33rd Symposium on Naval Hydrodynamics (which is unfortunately delayed because of the spread of COVID-19)

Fig. 3 China's AG600 seaplane (taken from TheGuardian.com)

3. Seaplane terminology

This section briefly describes the terminology used in seaplanes, which may not be familiar to all readers. The term "seaplane" can include "floatplanes," which are production aircraft fitted with twin floats; "flying boats" in which the hydrodynamic hull is built into the bottom of the fuselage, and "amphibians," which have landing gear to take off of land or water.

Figure 4 shows the geometry of a typical seaplane. Most seaplanes have a discontinuity in the bottom known as a "step" near the longitudinal center of gravity. This step permits the seaplane to rotate to an attitude required for takeoff. The most important characteristic of the step is its height. Large steps permit proper ventilation of the afterbody, but increase aerodynamic resistance. Although a transverse step is shown in Figure 4, there are many other types of step geometries that have been developed to improve ventilation characteristics or aerodynamic resistance, and these are discussed later in this article.

The area of the bottom forward of the step is known as the "forebody," and it is the primary load-carrying portion of the hull. The area of the bottom aft of the step is known as the "afterbody" and provides necessary hydrostatic buoyancy at low speeds but is typically out of the water near takeoff speed. The "sternpost" is the aft-most point of the hydrodynamic hull. The sternpost is not necessarily the back of the aircraft, as many seaplanes have a raised tail extending beyond the sternpost.

The angle measured from the projection of the forebody keel at the step to the sternpost is known as the "sternpost angle" σ. This is one of the most important features in determining the hydrostatic and hydrodynamic stability characteristics of the afterbody because it has a controlling influence of the pitching moments developed by the afterbody. There are large interactions between the "forebody wake," the flow pattern that forms at the step, and the afterbody. The "afterbody angle" (AA) is the angle the afterbody keel makes with the projection of the forebody keel and is less than the sternpost angle because of the effect of step height.

In section view, the "beam" or width of the planing surface is shown. The deadrise angle β is the angle between the horizontal and the bottom on the transverse plane. The deadrise angle has a large influence on impact loads during landing, hydrodynamic stability, and hydrodynamic resistance.

The region of the forebody bottom located within 1.5 beams of the step is known as the "forebody flat." It is critical to avoid curvature of the buttock lines in this region to prevent dynamic instabilities. Sometimes seaplane bottoms are "warped," meaning they have a linear increase in deadrise from the step forward. (See Savitsky 2012 for more details on warped hulls.)

As the seaplane moves through the water at forward speed, the "trim angle" τ, the angle of attack between the forebody keel and the level water surface varies with speed. In addition, the wetted area of the seaplane bottom will vary and so will the spray that is formed by the hull. The forward extent of the wetted area of the planing surface is known as the "spray root line," and this is also the origin of the

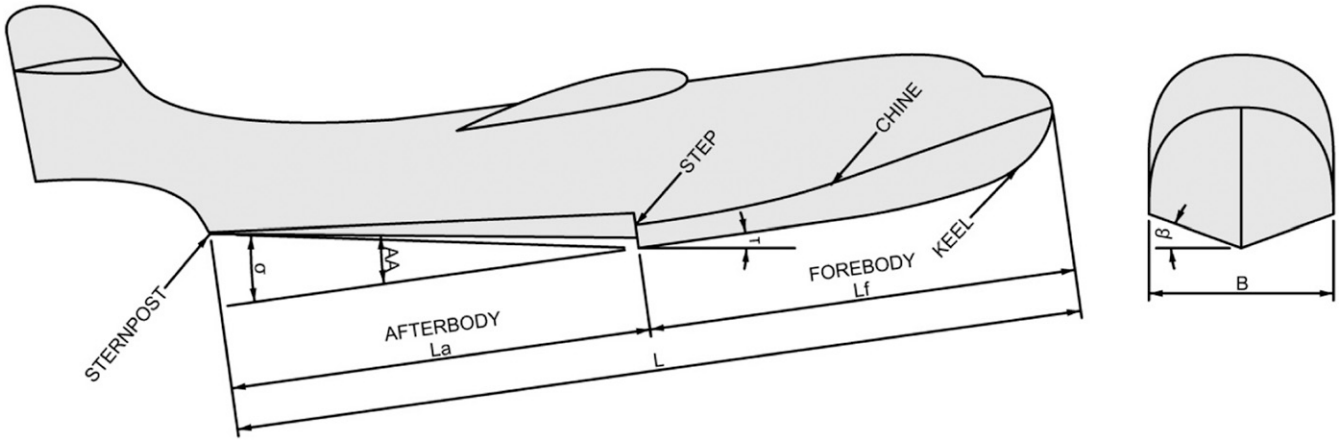

Fig. 4 Geometry of seaplane

spray that develops on the hull. (See Savitsky & Morabito 2011 for more on spray.) It is critical to avoid spray from the forebody damaging propellers or jet engines. The seaplanes shown in Figures 1 and 2 appear to have excellent spray characteristics, with the spray nowhere near the propellers; however, this is not always the case, as will be discussed later in this article.

4. Seaplane design concerns

The following list summarizes the main concerns that determine success or failure of the hydrodynamic design of seaplanes:

1) The hull meets static and damaged stability criteria;
2) engines produce enough thrust to get past hump speed and also to take off;
3) the hull does not have severe dynamic instabilities, such as porpoising or skipping;
4) spray does not damage propellers or wing structures; and
5) the bottom structure and airframe can withstand impact pressures and accelerations.

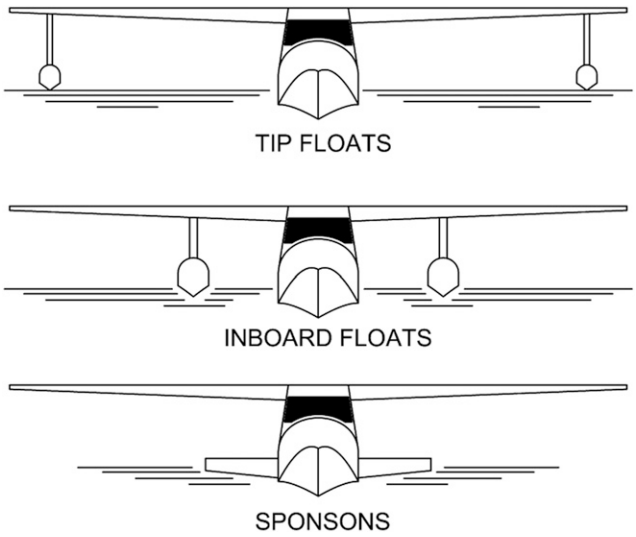

Fig. 5 Configurations of auxiliary floats (adapted from Korvin-Kroukovsky 1955)

4.1. Hydrostatic stability

The hydrostatic stability requirements for a seaplane include the following:

1) reserve buoyancy,
2) damaged stability, and
3) tip float sizing for flying boats.

In the United States, nonmilitary seaplanes must comply with the U.S. CFR Title 14: Parts 23 or 25, depending on the mission of the seaplane. Korvin-Kroukovsky (1955) and Diehl (1986) also provides some additional guidelines that are supplementary to the regulations but important to consider.

4.1.1. Reserve buoyancy. The CFR states that the hull of flying boats must provide a minimum of 80% reserve buoyancy. Korvin-Kroukovsky (1955) indicates that designing for 100% reserve buoyancy is good practice. Military aircraft have been built with reserve buoyancy of 65–130% on occasion. The reserve buoyancy is calculated based on the total immersed (watertight) volume of the hull. Watertight doors may be used.

4.1.2. Reserve buoyancy example. To determine the reserve buoyancy of the hull of a flying boat with a weight of 5000 kg and the hull displaces 9500 kg when immersed, the following equation should be used:

$$\frac{9500\ \text{kg} - 5000\text{kg}}{5000\ \text{kg}} 100\% = 90\%$$

The CFR requires that each main float of a floatplane has an 80% reserve buoyancy *based on the weight that it carries* in fresh water. For twin float seaplanes, the weight that the float carries is half of the weight of the aircraft.

The value of submerged displacement can easily be calculated with most hydrostatics software if a 3d model exists. In early design

stages, Korvin-Kroukovsky (1955) states that a block coefficient of .45 is typical for floats. (Thus, the volume can be determined by taking the product of .45 × length × beam × full immersed depth of the float.)

4.1.3. Watertight compartmentalization and damaged stability. Main floats for floatplanes are required to have a minimum of four–five watertight compartments of approximately equal volume, depending on the size of the aircraft. A minimum number of compartments are not specified for flying boat hulls.

Both flying boats and floatplanes are required to remain afloat and have a "reasonable assurance" against capsize if any two adjacent compartments of a main float or the hull are flooded. In some cases (per the CFR), only a one-compartment standard is required. Damaged stability calculations can be made using a compartmentalized 3d model in hydrostatics software capable of handling catamaran or trimaran configurations to account for twin floats or a main hull with tip floats.

4.1.4. Flying boat auxiliary floats. Flying boat hulls have narrow beam and high center of gravity, resulting in negative metacentric height and a lack of roll stability. As a result, they must be fitted with auxiliary floats. Figure 5 shows the three types ordinarily used: tip floats, inboard floats, and sponsons. Some high-performance aircraft that have anhedral (downward drooping) wings have the tip floats attached directly to the wings without the need for struts.

Auxiliary floats must

1) resist the natural upsetting moment created by the hull due to the high center of gravity,
2) resist wind heeling moments, and
3) provide margin of safety.

The auxiliary floats are often designed so that they are a few centimeters above or below the water surface at zero heel. This means that the seaplane will still have negative metacentric height at zero heel but will rapidly develop righting moment as the float is immersed.

Figure 6 shows a typical curve of heeling moment for a floatplane. The dashed line is the upsetting moment, calculated by running large-angle stability calculations, assuming there are no tip floats. This moment is destabilizing. The solid line is the righting moment, due to the tip floats. There is no righting moment until the float becomes immersed, around 1° of heel. Above this angle, the float provides a large, increasing righting moment. Once the float is fully immersed (above 8° on the diagram), there is very little change in righting moment until the wing becomes immersed

The CFR states that "auxiliary floats must be arranged so that when completely submerged in fresh water, they provide a righting moment of at least 1.5 times the upsetting moment caused by the seaplane or amphibian being tilted." This ratio can be determined from Figure 6 by comparing the upsetting moment and righting moment at 8°.

The factor of 1.5 is a simplification that includes the effects of wind heeling moments and the margin of safety. For large seaplanes, it may be necessary to exceed this value. The U.S. Navy previously had a more detailed criterion, which was discussed and analyzed by Carter (1947). The article shows a comparison of various transverse stability standards for flying boats and compares

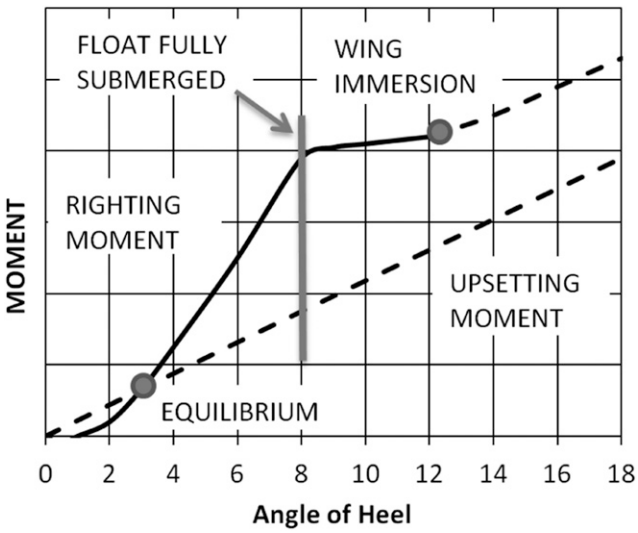

Fig. 6 Heeling moments versus angle of heel (adapted from Diehl 1986)

the standards with the opinion of the operators on how satisfactory the design is. The article also shows that the following guideline provides satisfactory tip float sizing (equation only works in U.S. customary units):

$$C\ \Delta_T = \Delta_O\left(h_e \sin\phi_1 + \frac{0.10 b_w}{\Delta_o/S} + 0.06\sqrt[3]{\Delta_O}\right)$$

where Δ_O is the static weight of the seaplane (lbf), Δ_T is the weight displacement of the tip float (lbf), C is the distance from the center of the tip float to the centerline of the seaplane (ft), ϕ_1 is the heel angle required to submerge the float, b_w is the wingspan (ft), S is the wing area (sq. ft), and h_e is the absolute value of the negative metacentric height at zero heel (ft).

4.1.5. Metacentric height for floatplanes. The spacing between the main floats of floatplanes will dictate the transverse metacentric height. The current CFR do not specify a minimum metacentric height for floatplanes. Diehl (1924, 1986) provides a guideline that is sometimes used in design, but the basis for this guidance is aircraft built before 1924, which are not similar to today's floatplanes. Korvin-Kroukovsky (1955) suggests the use of the (now outdated) CAA guidelines for metacentric height (equations only work in U.S. customary units):

$$\text{Longitudinal GM} \geq 6\sqrt[3]{\Delta_O}$$

$$\text{Transverse GM} \geq 4\sqrt[3]{\Delta_O}$$

where GM is metacentric height (ft) and Δ_O is the static weight of the seaplane (lbf).

4.2. Dynamic stability: Porpoising

Porpoising is a coupled oscillation in pitch and heave that can damage aircraft structures and make it impossible to achieve takeoff. Figure 7 shows a typical diagram of porpoising. In the diagram, the seaplane enters an uncontrollable oscillatory motion

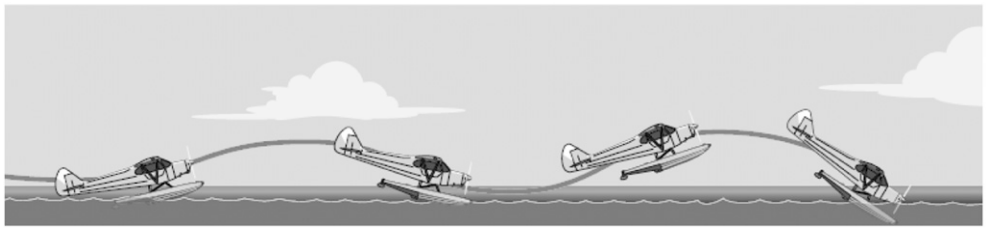

Fig. 7 Diagram of floatplane porpoising (Anon 2004)

with increasing amplitude, leading to an accident. Porpoising is a high-speed dynamic instability that is predicted by the lift coefficient of the planing surface $C_L = \frac{\Delta}{\frac{1}{2}\rho V^2 B^2}$ and the trim angle, as shown by Savitsky (1964) and confirmed by Celano (1998). Seaplane porpoising can result from the hydrodynamic characteristics of the forebody alone and forebody–afterbody interactions. Whereas a planing hull has only one porpoising limit—an upper limit of trim above which porpoising will occur at a given speed, a seaplane has two limits and must stay between them to prevent porpoising.

Figure 8 shows a typical plot of seaplane porpoising stability limits. The horizontal axis shows speed, and the vertical axis shows trim angle. It is necessary to stay between the two porpoising limits to prevent dangerous oscillations. The pilot has aerodynamic control at high speeds and can orient the seaplane between the limits if they are sufficiently separated. Poor designs have a very small stable region or none at all.

Porpoising is a result of large hydrodynamic forces combined with insufficient damping. In the case of planing hulls, this occurs at high speeds (low lift coefficients) and high trim angles, where a very small wetted area of hull generates a very large amount of lift. In seaplanes, it is more complex because of the effects of the forebody, the afterbody, the aerodynamic control surfaces, and the coupling between them all. Further (because the hydrodynamic forces are proportional to the square of speed) conditions that are stable at hump speed are not stable near takeoff. Davidson (1943) showed that

1) Both the *upper stability limit* and the *peak of the lower stability limit* increase with increasing sternpost angle.
2) The *upper limit* porpoising can be suppressed by effective ventilation of the afterbody near the main step.
3) The *lower* stability limit at *high speeds* is dependent on the forebody deadrise distribution, beam loading, and curvature of the buttocks.

Porpoising limits are often included in model test data of seaplanes.

4.3. Dynamic stability: Skipping

Skipping is an oscillation in heave that typically occurs during landings but has been observed during takeoff and also in steady speed towing tank tests. During a skip, the hull at high speeds will first be pulled downward into the water and then suddenly jump out of the water, sometimes causing a loss of control. Skipping is poorly understood at the present, but studies by Locke (1946) and Olson and Land (1948) indicate that it is related to AA, step height, and step ventilation.

Lorio et al. (2015) present a recent study on seaplane skipping. The purpose of the study was to isolate skipping (pure heave) from porpoising (heave and pitch) and rebound (an impact phenomenon). This was carried out by fixing the model in trim and running it in calm water, eliminating wave impact, rebound, or porpoising as possibilities.

Figure 9 shows a photograph of a typical run. The model was accelerated to a constant towing speed during the start of the run. As the model reached full speed, the stagnation line approached and then crossed the step. Once the stagnation line crossed the step, the following was observed, as illustrated in Figure 10

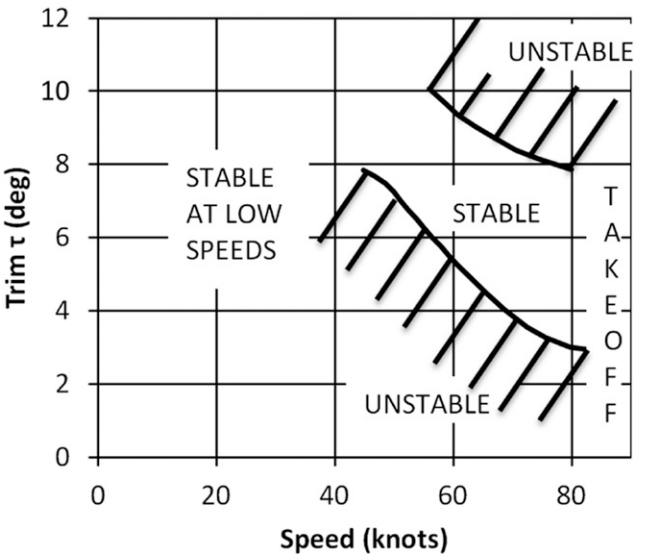

Fig. 8 Example trim limits of stability for a seaplane

Fig. 9 Photograph of skipping test (Lorio et al. 2015)

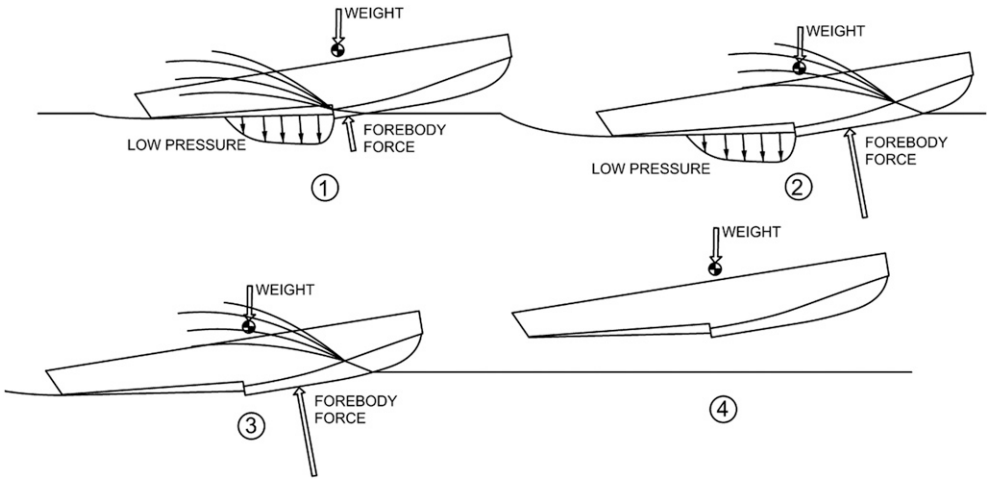

Fig. 10 Illustration of skipping (Lorio et al. 2015)

1) As the stagnation line crossed the step, the flow of air behind the step was blocked by spray and solid water. The pressure taps recorded strong negative pressures.
2) The hull moved downward, deeper into the water, increasing the wetted area of the forebody. The large increase in area increases the hydrodynamic lift force on the forebody, and the negative pressures on the afterbody continue to pull the hull deeper into the water.
3) The suction broke on the afterbody and the hull accelerated upward.
4) The hull left the surface of the water and upon its return repeated steps 1–4.

The tests were repeated a number of times, including the effects of variations in trim angle and step ventilation. Step ventilation eliminated the skipping tendency of this particular seaplane. The experiments provide strong indication of the importance of proper step ventilation and height.

4.4. Directional stability and turning

Seaplanes often require a water rudder (seen in Figure 11) because at low speeds, the aerodynamic forces on the tail are insufficient. Water rudders are especially common on single-engine craft as they cannot use variable thrust to provide a turning moment.

Fig. 11 Water rudders fitted to floatplane (anon., 2004)

Some designs have a directional instability known as "hooking." Davidson and Locke (1944) describes hooking as a very large unstable yawing moment at small yaw angles that can cause very rapid yawing or hooking on the seaplane. Because of the magnitude of the destabilizing yawing moments, it may not be possible to correct with unbalanced power or rudder force. Hooking can be detected in design stages with the use of static drift model tests, in which the model is towed at a range of yaw angles and yawing moments are measured. Pierson (1944) shows that severe yaw instabilities can be a result of unstable flow conditions around the afterbody sides and that skegs or side steps can improve directional stability.

4.5. Spray

Figure 12 demonstrates the spray patterns developed at different speeds for a large flying boat. Figure 12A shows the bow spray that occurs at low speeds (speeds where hydrostatic forces dominate). This spray can sometimes wet the cockpit windows with salt water during takeoff, obstructing visibility. Figure 12B shows the spray patterns at intermediate speeds near the hump speed. (This is the speed where the seaplane reaches its maximum trim angle and greatest hydrodynamic resistance.) In this photograph, spray is ingested into the propellers. This spray can cause severe propeller erosion. Salt water ingestion into turbojets is very problematic and must be avoided. Figure 12C shows the spray patterns at takeoff speeds. Typically, the spray is very large at this speed but is directed aft of the aircraft. Therefore, it is usually not a problem, unless tail surfaces become damaged.

Spray is most often an issue with flying boats as the propellers are relatively closer to the water surface and just outboard of the hull. Floatplanes are relatively higher off the water, and the spray from the floats usually does not enter the propellers or wet the cockpit windows. On both types of craft, there can be salt water corrosion problems with the spray impacting on the aft portions of the fuselage. Spray is made worse by having heavily loaded planing surfaces (high lift coefficients or large lift for a small bottom area). A variety of spray control devices have been fitted to aircraft with varying degrees of success.

Spray measurements are a part of typical seaplane tests, and using archival data, spray can often be estimated. In the absence of

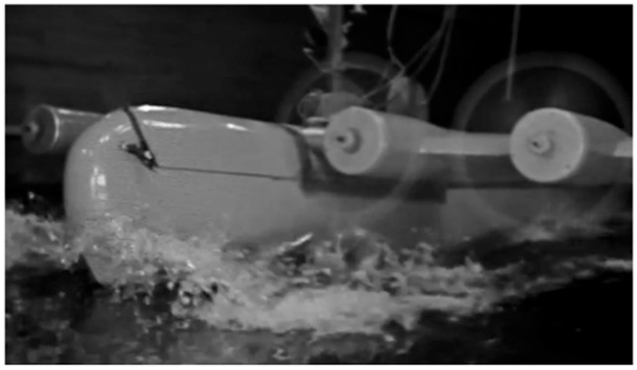

(A) Low Speed

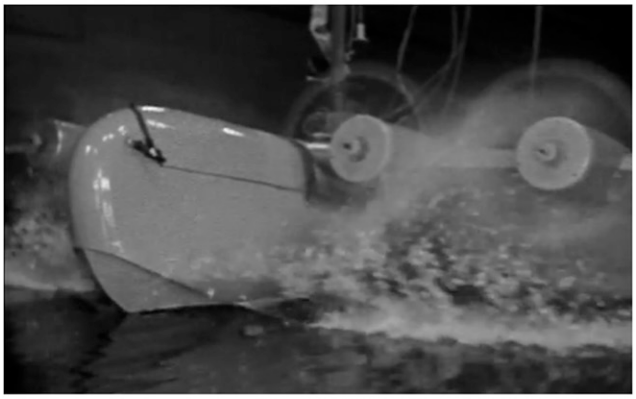

(B) Hump Speed

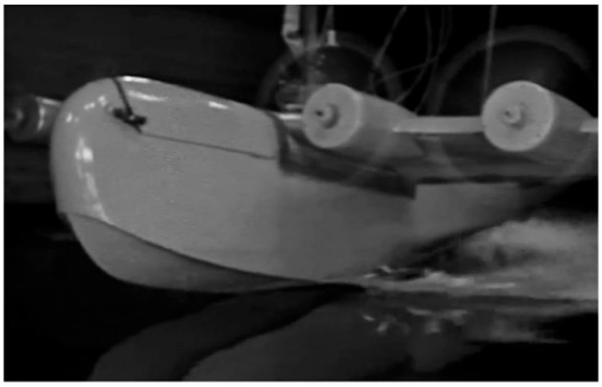

(C) Takeoff Speed

Fig. 12 Photograph showing spray patterns at various speeds (N.A.C.A. Tests of PB2Y-3)

archival data for a specific seaplane hull, the spray may be estimated using Savitsky and Breslin (1958), which was based on simplified "prismatic" planing hulls.

4.6. Impact

Impact accelerations during takeoff and landing are often the limiting factor for the operating envelope of the craft in a seaway. The hydrodynamic bottom pressures that lead to these accelerations requires a careful structural design of the bottom.

Calm water impact. The main factors that influence impact accelerations in calm water are given as follows:

1) Speed: Hydrodynamic impact pressures increase with the square of the speed.
2) Flight path angle: Larger flight path angle increases the relative velocity between the water and the bottom of the seaplane on impact.
3) Deadrise: Low deadrise presents a flatter bottom that will develop greater bottom pressures.
4) Trim: Higher trim angle (or angle of attack of the planing surface) will cause greater bottom pressures.
5) Beam: Wide bottoms have a larger area over which bottom pressures act. Because force is pressure times area, this larger beam results in higher impact accelerations.
6) Weight of seaplane: Because force equals mass times acceleration, accelerations will generally be lower for a seaplane with greater mass.

Unfortunately, many of these factors are already fixed by other areas of the design, including dynamic stability, takeoff thrust requirements, interior arrangements, and the lift-to-drag ratio of the wings. Some of the earliest studies of the calm water seaplane impact were carried out by Von Karman (1929) and Wagner (1931). NACA researchers continued this work in the 1940s and 1950s to a great deal of completeness. (See Milwitzky 1948 or Batterson & McArver 1950 for typical examples of theoretical and experimental work in this area.)

As designers in the 1950s pressed for higher speed designs (including supersonic fighter jet seaplanes and long-range bombers), they found that the impact accelerations were a primary limiting factor. Work was undertaken to provide skis that could be deployed from the bottom of aircraft (discussed later in the section on alternative hull forms) to reduce the hydrodynamic beam and consequently the impact forces.

Impact in waves. The effect of waves is to introduce a great deal of variability into the relative velocity of the hull and the water surface. Early studies modified the calm water approaches to include the presence of a sloped water surface on impact. Later studies on the impact basin (where seaplane models could be dropped to represent landing), as well as full-scale studies, focused on the more realistic problem of a seaplane landing and then decelerating as it moves through a series of waves.

Van Dyck (1958) noted that "in a given rough water landing, maximum load factors are rarely obtained on the first impact—or even during the second or third… Usually the impact which produces the maximum load occurs when the seaplane still has a fairly large forward velocity (below stall) but has rebounded from a wave system so that the pilot has little control over the aircraft."

Van Dyck, seeing that the theoretical predictions of the first impact were of little value and that full-scale or fully dynamic model tests in an impact basin were quite costly, proposed testing seaplanes in irregular seas at approximately 80% of the landing speed to determine the maximum impact. This is an effective and affordable test method in the towing tank. As the hull moves through the irregular seaway, its motions and forward speed are representative of what the craft would see during a decelerating landing on the third or fourth wave impact, where the pilot lacks control of pitch.

Empirical equations. Empirical equations were developed by Hugli and Van Dyck (1955) to estimate the impact accelerations of a seaplane. These may be useful in the design stages for trade-off studies of hull parameters.

$$\eta = 0.00825\ \gamma\ b\ V^2 \Delta_o^{-2/3} \left(1 - \beta/90\right)$$

where η is the impact acceleration at the center of gravity (g's), γ is the flight path angle (deg), b is the beam of the planing surface (ft), V is the landing speed (ft/s), Δ_o is the gross weight of the seaplane (lb), and β is the deadrise angle (deg).

Savitsky and Roper (unpublished analysis) note that this equation does not include trim; however, trim is limited by the sternpost angle of most seaplanes to 8–10°. Savitsky and Roper estimate typical flight path angle $\gamma = 5^0$ and also provided an empirical correction for impact accelerations in irregular waves based on unpublished data:

$$\gamma_e = 5^0 + \tan^{-1}\left(\frac{h_{1/3}\pi}{3L}\right)$$

where γ_e is an effective flight path angle in rough water, $h_{1/3}$ is the significant wave height, and L is the length of the seaplane.

CFR. Although the previous equations are useful qualitatively, CFR Title 14 part 23 and 25 include clear requirements for structural design of seaplanes. Equations are given to estimate the impact load factor (or acceleration) and the design bottom pressures to be used. The following equation is used to compute the load factors for the step landing case (other equations can include bow and stern impacts).

$$n_w = \frac{C_1 V_{SO}^2}{\left(\mathrm{Tan}^{\frac{2}{3}}\beta\right) W^{\frac{1}{3}}}$$

where n_w is the water reaction load factor (i.e., the water reaction divided by seaplane weight), C_1 is the empirical seaplane operations factor equal to .012 (except that this factor may not be less than that necessary to obtain the minimum value of step load factor of 2.33), V_{SO} is the seaplane stalling speed in knots with flaps extended in the appropriate landing position and with no slipstream effect, β is the angle of deadrise at the longitudinal station at which the load factor is being determined in accordance with figure 1 of appendix I of this part, and W is the seaplane landing weight in pounds.

The CFR equation does not include trim, flight path angle, and beam as parameters and therefore assumes a fairly typical seaplane design.

5. Early-stage sizing

This section discusses early-stage estimates of main hull parameters, such as length, beam, forebody length, sternpost angle, and step height. Guidance is provided about how each of these characteristics affects performance.

5.1. Length and beam of planing surfaces

The most important decision regarding overall performance of a seaplane is the size of the hull bottom to support a given load.

1) Hulls with high bottom loadings (i.e., too heavy a load on too small a planing surface) will have large spray, increased trim, and high resistance at hump speed.
2) The length-to-beam ratio of the hull is of primary importance for aerodynamic considerations, with higher length-to-beam ratio reducing parasitic drag of the aircraft.
3) The length and beam of the planing surface are driving factors for the volume of the fuselage on a flying boat, and therefore, its cargo-carrying and mission capabilities.

Before World War II, most flying boats had a length-to-beam ratio of 4–5 (see Figure 13, Grumman Goose). Seaplane floats made during the last 80 years often have length-to-beam ratios of 6–7. During the 1940s, extensive model testing and analytics allowed for designs with much higher length-to-beam ratios (and improved aerodynamic performance), such as the Martin P6M (seen in Figure 14). High L/B seaplanes, such as the Beriev BE-200 (seen in Figure 15) and AG600 (Fig. 3), are now in production.

5.1.1. Bottom loading. The Davidson load coefficient is often used to provide a guideline for the bottom loading of seaplanes with a wide variety of length-to-beam ratios, assuming that the length of the forebody is around the typical value of 55–60% of the overall length of the float.

$$K_2 = \frac{\Delta_O}{\rho g L^2 B}$$

where B is the hydrodynamic beam of the planing surface, measured at the chine and L is the length of the planing surface. As shown in Figure 4, "length" of the bottom is not the overall length of the seaplane but the length of the hydrodynamic hull (taken to the sternpost), which has some flexibility based on varying the tail overhang.

Δ_O is the load on the planing surface (half the weight of the seaplane for twin floats). Davidson and Locke (1944) found that hulls with varying length-to-beam ratios had similar resistance and spray characteristics when the loading coefficient and K_2 is kept constant. Stout (1950) provides the following recommendations for K_2, based on practical design experience with flying boats:

$K_2 = 0.018$ is optimum (light spray)
$K_2 = 0.022$ is maximum in design stages (heavy spray)
$K_2 = 0.025$ is maximum overload (excessive spray).

5.1.2. Forebody–afterbody proportions and effects. Although the forebody is often 55–60% of the overall length of the float for typical flying boats and floatplanes (Stout 1950), there is substantial room for flexibility on this value in design. Haar (1952) tested hulls

Fig. 13 Typical pre-war flying boat(Grumman G-21 Goose)

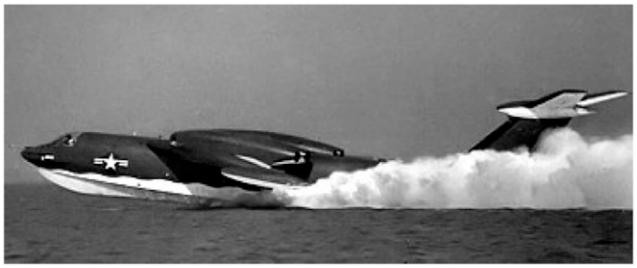

Fig. 14 1950s long-rang bomber (Martin P6M)

with forebody lengths ranging from 33% to 60% of the length of the float, showing that a wide range is possible. Long afterbodies reduce the upper porpoising limit because they contact the surface at lower trim angles; however, this can be remedied by increasing the sternpost angle.

Spray characteristics are mainly related to forebody load, and so shortening the forebody for the same Davidson load coefficient K_2 will result in increased spray. For hulls with forebody lengths lower than the typical 55–60%, Parkinson's (1943) forebody load coefficient provides a useful guide.

$$k = \frac{\Delta_O}{\rho g L_f^2 B}$$

where Parkinson recommends the following:
Excessive spray $k = .0975$,
heavy, but acceptable for overload $k = .0825$,
satisfactory for normal operation $k = 0.0675$, and
extremely light spray $k = 0.0525$.

5.1.3. Beam loading. Beam-based coefficients are often used in seaplane references because although the wetted length varies with speed, the beam remains essentially constant. Most seaplane literature from NACA uses the load coefficient C_{Δ_O}, which is based on beam. This coefficient can be related to K_2 as follows:

$$C_{\Delta_O} = \frac{\Delta_O}{\rho g B^3} = K_2 \left(\frac{L}{B}\right)^2$$

Most of the guidance on seaplane loading, C_{Δ_O}, during the prewar period is based on the assumption that the length-to-beam ratio is somewhere around 6, and therefore, it is important not to use these pre-war design guidelines for craft with very high length-to-beam ratio.

Fig. 15 Modern production "water bomber" (Beriev Be-200)

5.2. Step Design

The step allows flow to cleanly separate off the forebody at speeds above hump and permits the aircraft to rotate to a trim angle to allow takeoff. The step is typically located .2 to .4 beams aft of the center of gravity. Placing the step too far forward will cause the seaplane to run at too high a trim angle or balance on the afterbody at high speeds. Placing the step too far aft will prevent the seaplane from rotating to take off.

Larger step heights are typically better for hydrodynamic stability but worse for aerodynamic resistance. It has been observed that hulls with too small a step tend to "skip." The airflow becomes blocked aft of the step creating a low-pressure region that causes the hull to be pulled downward. When the suction is broken, the hull jumps out of the water. This happens most often on landing, but sometimes during takeoff and has been observed in full scale and in towing tanks. The effects of step height and AA also control the porpoising behavior of designs.

Locke (1946) investigated the skipping characteristics of full-scale seaplanes, based on pilot input, and found that increased step height, reduced beam loading C_{Δ_O}, and reduced sternpost angle σ all tend to improve performance. This study was limited to a length-to-beam ratio of 6 (based on existing designs) and can produce step heights that are too small for high L/B designs.

As work was going on to explore large variations in the length-to-beam ratio, Olson and Land (1948) prepared systematic model tests of afterbody length, AA, and step depth to study the effects of these parameters on the takeoff and landing stability of seaplanes (Fig. 16). From these tests, they derived a formula relating these parameters and compared it with the results of model-scale landing tests of a variety of hulls previously tested by NACA. Their formula (in the notation used in this article) is as follows:

$$h_{\%b} \geq 0.59 \frac{L_a}{b} \mathrm{AA}$$

where $h_{\%b}$ is step height in a percentage of beam, L_a is the length of the afterbody (meters), b is the beam of the planing surface (meters), and AA is the afterbody angle (degrees, see Figure 4) (this equation can use meters or feet because they cancel).

Step height example:

Estimate the minimum step height for the following seaplane using Olson and Land's (1948) criteria.

$L_a = 12.8$ m $b = 3$ m
AA $= 5.5°$ $\sigma = 7.3°$ $\Delta_O = 56{,}000$ kg
Ans: $h_{\%b} \geq .59 \frac{L_a}{b} \mathrm{AA} \geq .59 \frac{12.8m}{3m} 5.5 \text{ deg} = 13.8\%$

5.2.1. Step planform shape. Many seaplane floats have transverse steps; however, it has been shown that adding a "Vee-Step," as shown in Figure 17, can improve step ventilation and performance. Savitsky (1951) showed that for prismatic planing hulls, 30° and 45° Vee step angles had a higher lift-to-drag ratio than a transverse step. Van Dyck (1954) confirmed that for seaplane hulls, the 45° angle resulted in the minimum skipping tendency (evidence of good ventilation), did not affect directional stability, and had the least resistance of the configurations at hump speed.

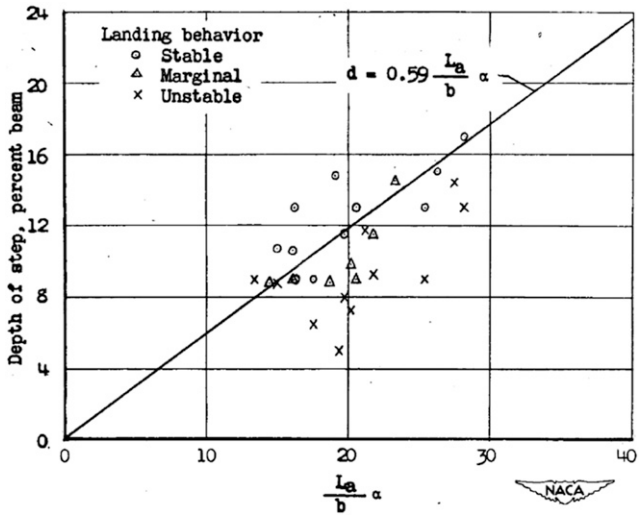

Fig. 16 Guidance relating AA, afterbody length, step height, and beam, based on takeoff and landing tests of various models at NACA (Olson & Land 1948)

The "Vee step" used on seaplanes differs from the re-entrant step advocated by Clement for use on stepped planing hulls (See Clement & Hoyt [2008] or Clement 1969). Re-entrant steps have the point facing forward and are designed to allow for the addition of longitudinal camber (hook) near the step, increasing the lift coefficient of the planing surface. Because of the poor ventilation characteristics of these steps, they must be fitted with vents aft of the step to prevent dynamic instabilities. Re-entrant steps have not, to the author's knowledge, been successfully used on seaplanes and do not seem to be appropriate. The seaplane requires very low lift coefficients from the planing surface on takeoff (light load on the water from aerodynamic lift, combined with high speeds), and so the addition of camber at the step is strongly discouraged.

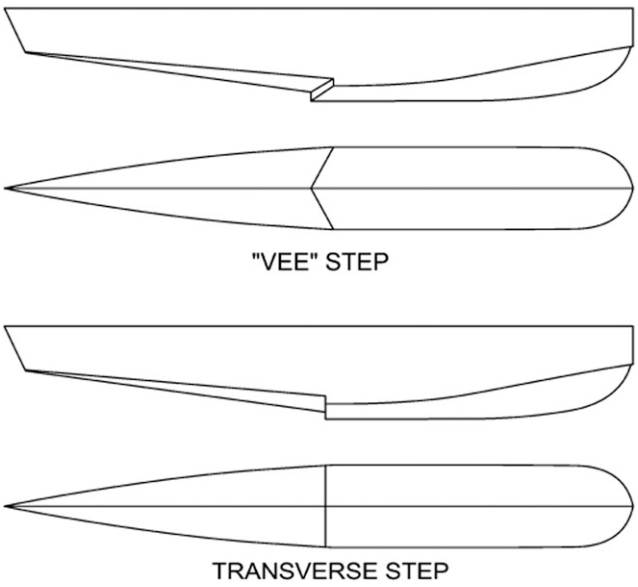

Fig. 17 Transverse and Vee step configurations

5.2.2. Step fairing. Fairing the step can reduce the aerodynamic resistance; however, care must be taken to ensure the water breaks cleanly from the step. If the flow does not cleanly separate, there will be dynamic instabilities and increased resistance. Figure 18, taken from Smith and Allen (1954), shows a variety of step fairings that have been used, sorted with the most aerodynamic resistance at the top and least at bottom. The straight fairing has the least resistance; however, this is the most unlikely for the water to separate from and least likely to naturally ventilate.

5.3. Deadrise angle and warp

Typical seaplanes have deadrise angles around 20° at the step. Increasing deadrise makes the bottom a less effective lifting surface, resulting in reduced impact accelerations during landing and in waves. Increased deadrise also increases resistance of the hull because more wetted area is required to generate a given lift. Reducing deadrise below 20° increases the lower limit of porpoising and is usually not recommended.

It is essential to provide straight buttock lines on the forebody in the vicinity of the step. Convex curvature in this area results in dynamic instabilities. The hull naturally will have more curvature toward the bow, but convexity is still to be minimized.

The bottom often has a "forebody flat," which is a region ahead where the buttock lines are kept completely straight. The flat can be developed by either maintaining a constant deadrise or by a linear warping (i.e., a linear increase in deadrise as a function of distance forward of the step). Warp has been shown to reduce the lower limit of porpoising at high speeds for high–length-to-beam ratio hulls, increasing the region of safe operation. Figure 19, taken from Stout (1950), provides a recommendation on the amount of warp in the forebody flat. A high–length-to-beam ratio hull, with a forebody length-to-beam ratio of 8 should have roughly 5° per beam of warp. Thus, if it is a 20° deadrise at the step, it will have 25° one beam forward of the step.

5.4. Sternpost angle

Sternpost angle (labeled σ in Figure 4) affects the resistance, porpoising stability limits, and spray characteristics. Dathe and de Leo (1989) lists the effects of changing sternpost angle.

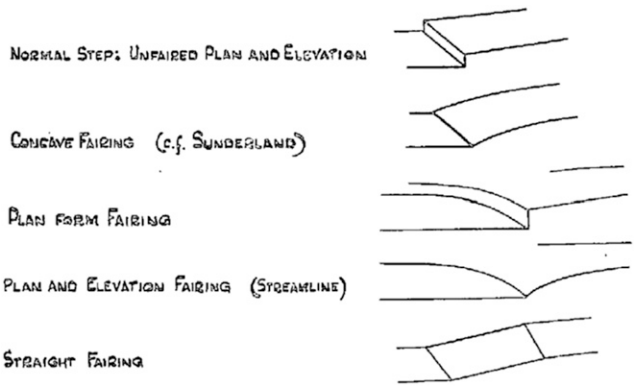

Fig. 18 Step fairing options—highest drag top, lowest drag bottom (adapted from Smith & Allen 1954)

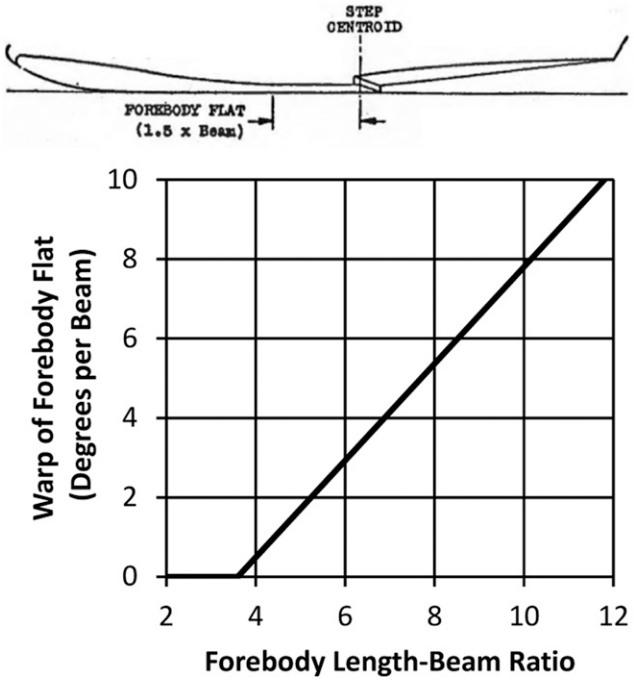

Fig. 19 Recommended linear variation in deadrise forward of the step in degrees per beam of the forebody flat to maintain lower limit stability (Stout 1950).

Increased Sternpost Angle:

1) Reduces afterbody interaction, raising the upper porpoising limit (good);
2) reduces afterbody damping, raising lower porpoising limit at hump speed (bad);
3) causes the seaplane to run at higher trim at lower speeds, increasing spray (bad);
4) may cause higher impact accelerations because of higher trim (bad); and
5) may allow the seaplane to rotate to a more favorable takeoff orientation (good).

It is not possible to provide a general guide to sternpost angle, other than to note that typical seaplanes that have been built have sternpost angles in the range of 7–9° (Locke 1946; Hugli & Van Dyck [1955]). The previous guidance on step height may be of some aid in relating sternpost angle to step height.

5.5. Alternative Hull forms

The two most promising alternatives to the conventional seaplane hulls described earlier are the "planing tail" and "hydro-ski" seaplane concepts. The advantages and disadvantages are discussed in the following text.

5.5.1. Planing tail seaplanes. Figure 20 shows a photograph of a planing tail seaplane. The primary difference between a conventional seaplane and a planing tail seaplane is the step height is substantially higher and the afterbody provides very little hydrostatic support. At high speeds, the hull rides on two points—the forebody planing surface and the aft portion of the afterbody,

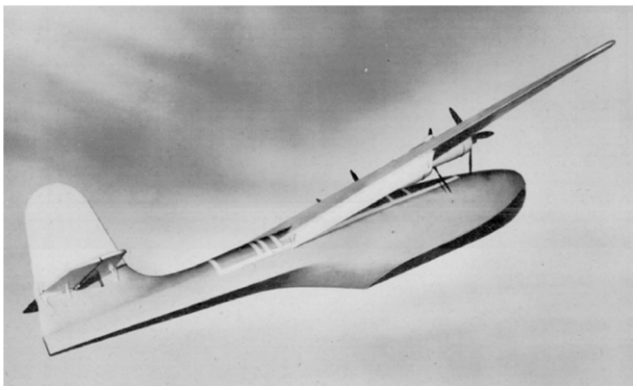

Fig. 20 Planing tail seaplane (Suydam 1952)

located under the tail. Planing tail seaplanes have larger static trims and less internal volume than conventional seaplanes. However, they have better step ventilation, reduced aerodynamic resistance due to the long fairing of the step, and less hydrodynamic resistance (Suydam 1952). Furthermore, the planing tail seaplane does not usually suffer from upper limit porpoising (which is a result of the afterbody) or skipping (which is a result of poor step ventilation). Suydam's study showed that the planing tail seaplane had a much lower lower limit for porpoising stability, so a much wider range of trim angles were permissible.

For these reasons, planing tail designs are very popular today for light one- or two-passenger recreational aircraft, where cargo-carrying capacity is not important. They are also an excellent choice for unmanned aerial vehicles.

Much of the same design guidance discussed previously applies to planing tail seaplanes, except the use of the Davidson load coefficient, $K_2 = \frac{\Delta_O}{\rho g L^2 B}$, because of differences in the afterbody. Instead, we would recommend using Parkinson's (1943) forebody load coefficient $k = \frac{\Delta_O}{\rho g L_f^2 B}$, discussed earlier in the section on forebody–afterbody proportions.

5.5.2. Hydro-ski seaplanes. High-speed aircraft, such as supersonic fighter jets, are designed to have a very small wing area to reduce parasitic drag at high speeds. As a result, they must take off and land at higher speeds. Because hydrodynamic impact pressures typically vary with the square of speed, impact accelerations become problematic for high-speed seaplane designs. Figure 21

Fig. 21 Sea Dart—hydro-ski fighter jet (photo courtesy of Smithsonian National Air and Space Museum)

shows a photograph of Sea Dart, an experimental supersonic fighter jet seaplane. To reduce the landing impact loads, two narrow hydro-skis were deployed from the bottom. Reduction in beam of the planing surface reduced impact loads. In addition, the hydro-skis could be mounted on shock-absorbing struts.

Hugli and Van Dyck (1955) prepared a limitation analysis, comparing the resistance of hydro-ski seaplanes and conventional seaplanes at similar values of impact accelerations. This study yielded a useful plot to estimate where each type of hull is appropriate (Figure 22). The figure shows the thrust-to-weight ratio required for takeoff as a function of volumetric Froude number based on static load and getaway speed. The plot shows that at high Froude numbers, the hydro-ski alighting gear has substantially lower thrust requirements. The reason for the increased thrust requirement for hulls at higher volumetric Froude numbers is the need for ever increasing deadrise to prevent impact accelerations. By contrast, hydro-skis can be made much narrower to limit impacts.

Since the 1950s, there has been very little development in hydro-ski seaplanes. This is likely because few jet fighters require the ability to take off and land from water. Thus, hydro-ski seaplanes are a feasible technical solution for which there is little need.

A thorough summary on the hydrodynamic design of hydro-ski planes is provided in a two-part technical report by Pepper and Kaplan (1966, 1968). These reports (more than 350 pages total) should provide the design data necessary for a very detailed analysis.

$$F_{\nabla_G} = V_G \Big/ \sqrt{g\nabla_O^{1/3}}$$

6. Performance predictions

The main topic of interest in performance predictions is to determine whether the engine thrust can overcome the resistance and allow takeoff speeds to be reached, and whether the porpoising characteristics of the hull will permit takeoff without a loss of control.

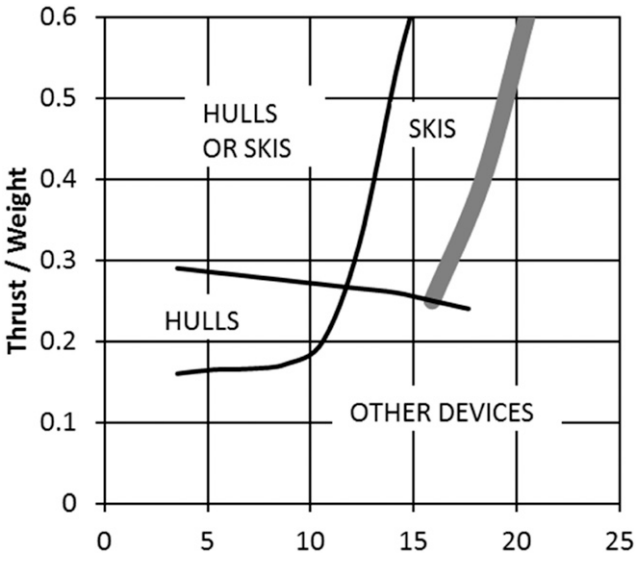

Fig. 22 Regions for alternative hull forms—thrust-to-weight ratio required for takeoff for hulls and hydrofoils with equivalent impact accelerations L/B = 15 (Hugli and Van Dyck 1955)

The thrust of the engines must overcome both the aerodynamic and hydrodynamic resistance of a seaplane. Thus, a brief discussion of aerodynamics is in order. This is necessarily simplified for convenience.

6.1. Simplified aerodynamic factors

During takeoff, the wings provide increasing lift with increasing speed, and therefore, the load supported by the water varies with speed. It is often assumed in early design that the wings remain at a constant angle of attack (controlled by the pilot at speeds where aerodynamic lift is significant), and so the lift by them varies parabolically, until at the takeoff speed V_o when the lift is equal to the weight of the seaplane, and there is no load on the water. This parabolic unloading is described by the following equation:

$$\Delta = \Delta_o\left(1 - V^2/V_G^2\right)$$

where Δ_O is the static weight of the seaplane (N or lbf), Δ is the load on the water at any given speed (N or lbf), V_G is the getaway or takeoff speed (m/sec), and V is the speed (m/sec).

During takeoff, the wing is assumed to be operating at its maximum lift coefficient. The aerodynamic lift coefficient is defined as follows:

$$C_{LA} = \frac{L_A}{\frac{1}{2}\rho_A V^2 S}$$

where L_A is the aerodynamic lift (N), ρ_A is the density of air (kg/m^3), S is the wing planform area (m^2), and V is the speed (m/sec).

The maximum lift coefficient occurs just before stall and is often increased by 1) the use of flaps at the trailing edge, which increases the camber of the section and 2) leading edge slats, which control the boundary layer, increasing the angle of attack at stall. Figure 23 shows some typical high-lift configurations. It should be recognized that some of the most complex configurations will not be feasible for small aircraft. The following table of 2-D maximum lift coefficients is developed from data summarized by Kroo and Shevell (2006).

Configuration	C_{LAmax}
Flaps Retracted	1.3 - 1.6
Single Slotted Flap	2.0 - 2.5
Single Slotted Flap + Leading Edge Device	2.3 - 2.5
Double Slotted Flap + Leading Edge Device	2.2 - 3.0
Triple Slotted Flap + Leading Edge Device	2.5 - 3.0

The stall speed may be estimated from the maximum lift coefficient as follows:

$$V_{\text{STALL}} = \sqrt{\frac{\Delta_o}{\frac{1}{2}\rho S C_{\text{LAmax}}}}$$

The takeoff or getaway speed is taken to be about 10% higher than the stall speed.

$$V_G = 1.1 V_{\text{STALL}}$$

The aerodynamic drag is given as follows:

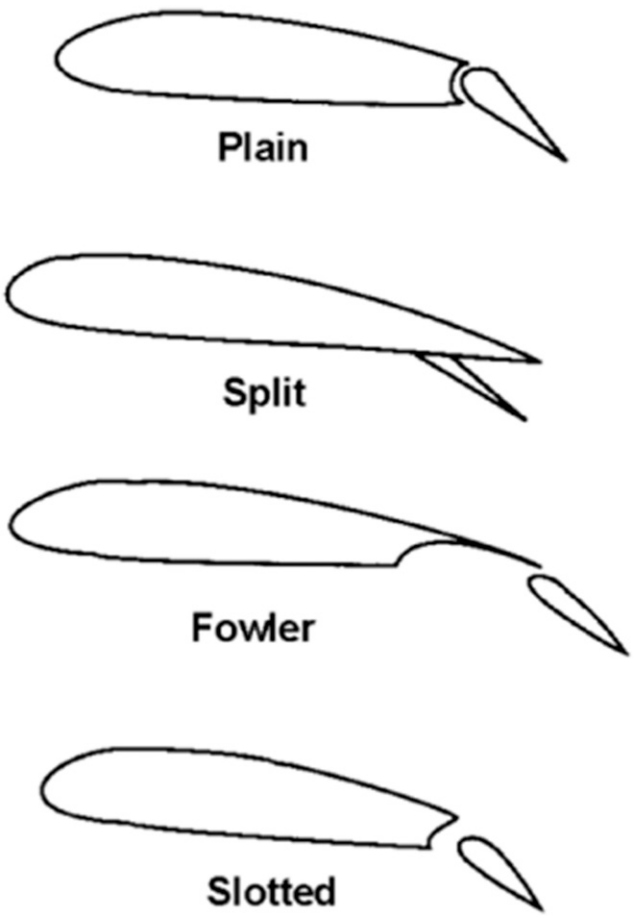

Fig. 23 Typical high-lift configurations (NASA)

$$D_A = C_{\mathrm{DA}} \frac{1}{2} \rho_A V^2 S$$

From lifting line theory, we can estimate the induced drag and add it to the parasitic drag as follows:

$$C_{\mathrm{DA}} = C_{\mathrm{Dp}} + \frac{C_{\mathrm{Lmax}}^2}{\pi \ \mathrm{AR} \ e}$$

where D_A is the aerodynamic drag (N), C_{DA} is the aerodynamic drag coefficient, C_{Dp} is the parasitic drag coefficient (In the absence of aerodynamic drag predictions, $C_{\mathrm{Dp}} = .025$ is a typical value based on Hugli and Van Dyck [1955].), C_{LAmax} is the maximum lift coefficient, AR is the aspect ratio $= \frac{\mathrm{Span}^2}{\mathrm{Wing\ Area}}$, and e is the planform efficiency factor.

($e = 1.0$ for elliptical lift distribution and $\sim .8$ for average wings.)

From these simplified aerodynamic estimates, it is possible to determine the aerodynamic resistance as a function of speed and the load on the water in early stages of design.

6.2. Hydrodynamic resistance characteristics

Figure 24 shows a typical plot of seaplane resistance data from a model test. The curve labeled "load" is the weight supported by the water. The loading at zero speed is equal to the displacement of the seaplane Δ_o. The plot shows curves of trim and of change in draft. The seaplane is free to heave and trim.

At low speeds, the aerodynamic forces are small, and the hull behaves similar to a boat. Initially, the change in draft is negative, meaning the hydrodynamic forces act to pull the hull downward. As speed increases, there begins to be a hydrodynamic lift force that causes the center of gravity of the seaplane to rise above the still water position.

Figure 24 shows a speed where there is a maximum in both trim and resistance. This is known as "hump speed." It is imperative that the aerodynamic thrust exceeds the resistance at hump speed, with a margin to allow acceleration. Beyond hump speed, the aerodynamic lift increases, reducing the load on the water (and consequently the resistance) to zero.

Figure 24 also shows fixed-trim resistance. At speeds above hump, there is often sufficient aerodynamic control for the pilot to set the trim angle. Therefore, the seaplane is no longer free-to-trim, but responds to control.

6.3. Hydrodynamic resistance prediction

Currently, the most reliable method to predict the hydrodynamic resistance is through specific model tests on the actual design. There are two commercial facilities in the United States capable of these tests, Tank 3 at Stevens Institute of Technology in Hoboken, NJ, and the high-speed towing tank at Carderock in Bethesda, MD. Lower speed tanks, such as the one at the U.S. Naval Academy, can do the tests, provided sufficiently small models. In early design stages, specific model tests are not available, and so other estimates may be used. These methods are reviewed in the following text.

Substantial effort was put into development of analytical methods for predicting the hydrodynamic performance of the forebody of seaplanes. The popular Savitsky (1964) method for planing craft is based on this research, and it can be also applied to the forebody of the seaplane. Unfortunately, the afterbody interaction has never been characterized to an extent where there is confidence in the results when applied to seaplanes. Therefore, the Savitsky method remains an interesting process but not useful to the immediate problem.

Computational fluid dynamics codes are rapidly developing in capability. As researchers continue to invest time and effort, they are approaching a point where they will become very useful in this field. The computations are very complicated because of the porpoising and skipping instabilities, the spray interaction, and the resistance of the afterbody when it is partially immersed in the wake of the forebody. Qiu and Song (2016) have shown how computational methods can be used to improve step design, but the dynamic stability continues to be an area of development. As with physical model tests, the computational predictions require a hull design in advance, which requires some preliminary sizing, such as the methods summarized here.

Early-stage hydrodynamic resistance prediction can be accomplished before the final hull parameters are set, using one of the many standard series of seaplane tests. Four extensive standard series are listed:

1) Tomaszewski 1946, Hydrodynamic Design of Seaplane Floats. Ministry of Supply. Aeronautical Research Council Current Papers. Royal Aircraft Establishment Report No. Aero 2154.
2) Hugli and Axt (1951) Hydrodynamic Investigation of a Series of Hull Models Suitable for Small Flying Boats and Amphibians. NACA Technical Note 2503.

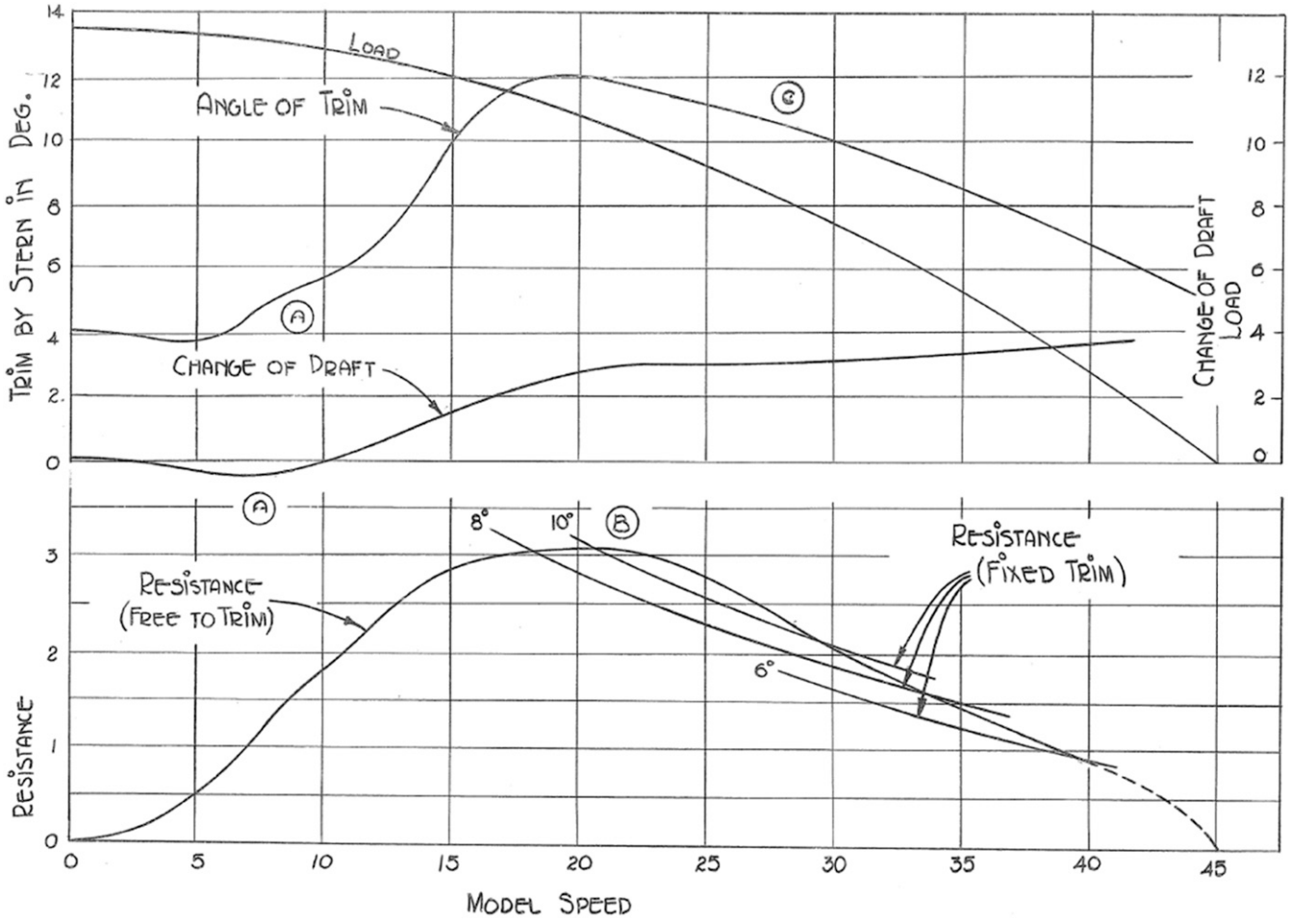

Fig. 24 Typical resistance test data (Korvin-Kroukovsky 1955)

3) Locke 1947, A Collection of the Collapsed Results of General Tank Tests of Miscellaneous Flying-Boat-Hull Models. NACA Technical Note No. 1182.
4) Strumpf 1947, Model Tests on a Standard Series of Flying-Boat Hulls. Experimental Towing Tank Report No. 325, Stevens Institute of Technology, Hoboken, NJ.

Most of these studies are from the immediate post–World War II era. The emphasis on most of the more recent studies (last 65 years!) has been on specific point designs, rather than design space exploration. If your design happens to be similar to one of these point designs that has been extensively tested, they are a great source of information. One of the best ways to search this information out is through the NASA Technical Reports Server.

Many of the standard series listed previously present data using the "Stevens Collapsed Data Set," (Fig. 25). The reader should consult Locke (1944) or deCallies (1958) to understand the coefficients used. I will note that the deCallies (1958) report is an excellent summary of seaplane aerodynamics, and I highly recommend it in addition to this article.

These standard series charts can be used to iterate to a design that meets the requirements while having satisfactory porpoising and spray characteristics. Once this iteration is complete, more expensive prediction methods, such as CFD or physical model tests, should be used.

6.4. Combining aero- and hydrodynamics

Figure 26 shows the resistance components of a seaplane used for takeoff calculations. The figure shows the aerodynamic drag, which increases roughly with the square of the speed; the hull drag, which is a maximum at "hump speed" and then diminishes to zero at takeoff; and the total drag, which is the sum of those two components. Also shown is the propeller thrust. It is important that the thrust available exceeds the resistance

The takeoff time can be estimated as follows:

$$t = \int_{o}^{V_G} \frac{M}{(T-R)} \mathrm{dV}$$

where T is the propeller thrust, M is the mass of the seaplane (weight/G), and R is the total resistance.

The above equation can be evaluated numerically using a method such as Simpson's rule. The triangles between the curves in Figure 26 correspond to seconds that it takes to accelerate and take off. This is an alternate graphical method to determine takeoff time. Parkinson (1948) provides a demonstration of this process.

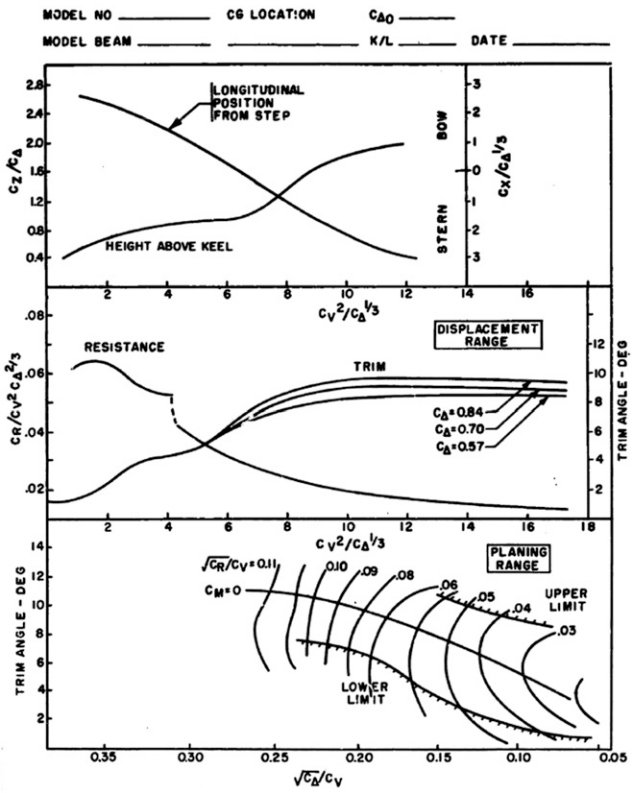

Fig. 25 Stevens collapsed data set (deCallies 1958)

7. Design process

Design is an iterative process. Given a weight, it is possible to determine, based on the information provided in this article, an estimate for the design parameters such as length, beam, deadrise angle, sternpost angle, and step geometry. From these parameters, it is possible to identify an appropriate standard series and select a suitable hull. With basic aerodynamic information such as the wing area and maximum lift coefficient, an estimate for the getaway speed can be made. Knowing the getaway speed and having the standard series, it is possible to establish the resistance, porpoising, and spray characteristics of a design. This design may then be compared with the design requirements (such as volumetric capacity, range, and payload) and iterated as necessary.

Although the aforementioned process covers the aerodynamic and hydrodynamic considerations, it does not include information such as the aircraft structural weights and engine availability. Such information may be found in books on aircraft design; however, the structural weights for seaplanes are an elusive subject. Cooper and Kennell (2015) provide an extensive data set of seaplane principal characteristics, including weight, length, wing area, takeoff distance, stall speed, cruise speed, and maximum speed. Figure 27 shows an example of one such plot from Cooper and Kennell (2015). Locke (1953) provides a reference with detailed information on weights. The structural weights for riveted aluminum hulls in this reference may not be too far off, but obviously electronics systems and engines would not be accurate from a report of this age.

Regardless of the complexities of design, it is important to remember that the best seaplane takes off at an extremely low speed and have a large thrust margin. Operating in waves at speeds in excess of 100 miles per hour during long takeoff runs can put extreme loads on the airframe and crew.

8. Model testing procedures

Upon completion of the conceptual design using the methods discussed earlier in this article and having made performance predictions using archival data, physical model testing is recommended. This section discusses some of the different types of model tests that can be conducted, starting with the types of models to be tested.

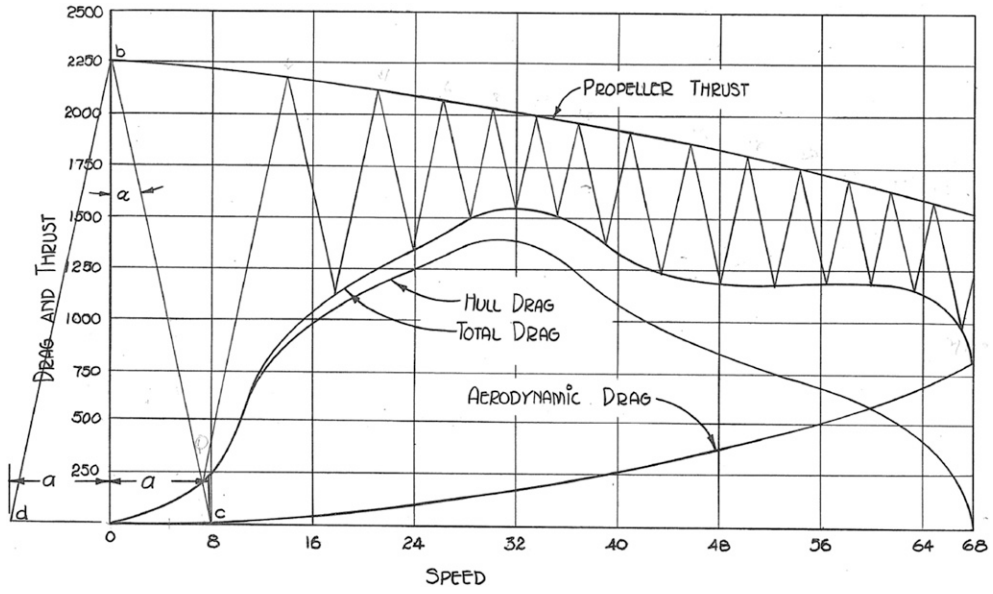

Fig. 26 Typical takeoff calculations (taken from Korvin-Kroukovsky 1955)

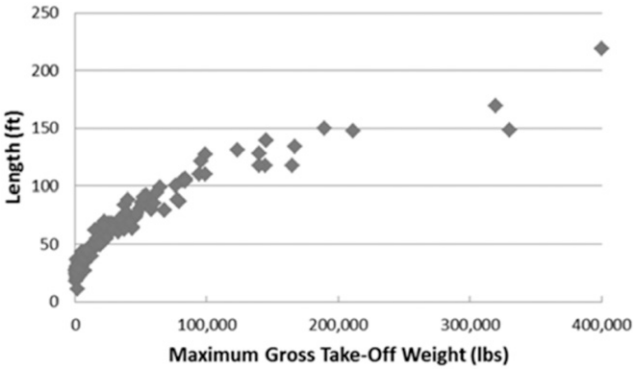

Fig. 27 Example plot of parametric data available in Cooper and Kennell (2015).

8.1. Model types

There are four main types of seaplane towing models available, listed in decreasing order of cost:

1) Remote-controlled, powered, dynamically similar models (Fig. 28). These models are for observations of fully dynamic seaplane behavior, including takeoff, landing, maneuvering, and impact in waves. They have excellent demonstration value and will show key dynamic instabilities. Tests made outdoors are subject to nature's variations in wind and wave conditions, making repeatable measurements problematic. These are the most expensive and complex models to build.
2) Powered dynamically similar towing models (Fig. 29) are intended for straight-line towing tanks. The models are fixed in heel, and the flap positions are set prior to each run. As a result, they cannot represent dynamic behavior outside of the vertical longitudinal plane. Use of a towing basin permits systematic variation of test parameters and repeatable results. Data recording does not have to occur on the model, rather instrumentation cables transmit the signals to the towing carriage. The use of propellers simulates their effect on wing lift, and identifies more easily spray interaction with propellers.
3) Unpowered towing models with wings (Fig. 30) are substantially less expensive than powered models. They permit measurements of the total resistance, trim, heave and accelerations in waves. They do not model the slipstream interaction with the wings. Often times, leading edge slats are added to the wings to allow the wing lift at the low model Reynolds numbers to appropriately represent the full-scale lift. Getting this exact requires trial and error, and can be time consuming. The need for similar aerodynamic characteristics at substantially different Reynolds numbers is a problem for all models with wings.
4) Hull-only towing models (Fig. 31) are used to characterize the hydrodynamic properties of a design without the interaction of wings and propulsion. Trimming weights, located fore and aft, are used to represent aerodynamic pitching moments because of the tail. Unloading (either with springs, or with counterweights) represents the wing lift. Testing a wide variety of loadings allows for a more general description of the hydrodynamic characteristics, which can be paired with any set of aerodynamic coefficients, and a wide range of gross weights in the future. Seaplane standard series, are developed using hull-only models, providing flexibility for concept designs.

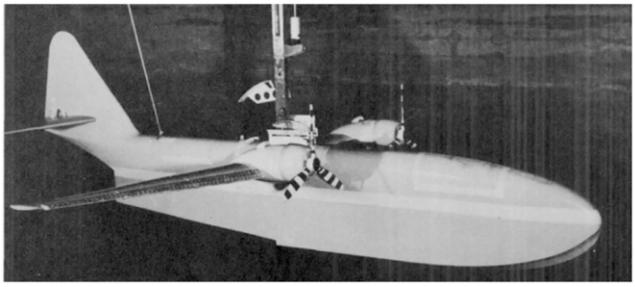

Fig. 29 Powered dynamically similar towing model (Parkinson 1955)

8.2. Dynamic similarity

The scale ratio λ is defined as the ratio of ship length to model length:

$$\lambda = L_S / L_M$$

Because of the need to properly model the wave making component of resistance during takeoff and landing on water, Froude scaling must

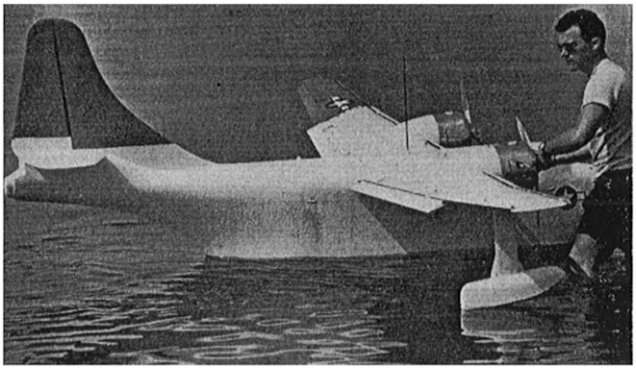

Fig. 28 Remote-controlled powered dynamically similar model (Stout 1950)

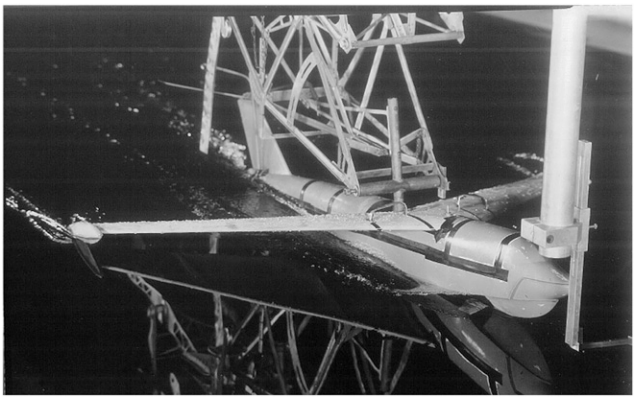

Fig. 30 Unpowered towing model with wings (courtesy of Davidson laboratory, stevens institute of technology)

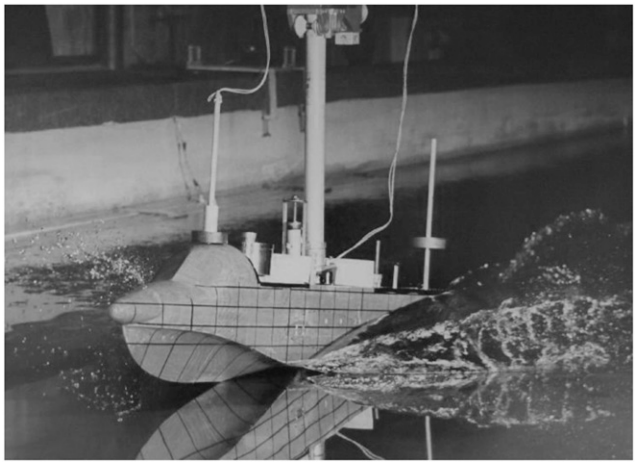

Fig. 31 Hull only, with mechanical wing unloading (courtesy of Davidson Laboratory, Stevens Institute of Technology)

be used. The most fundamental aspect is that the speed of the model is related to the speed of the ship by the square root of the scale ratio:

$$V_M = V_S \Big/ \sqrt{\lambda}$$

Stout (1950) provides a discussion of the other relations required for dynamic similarity, and the results are summarized in in the table given as follows. Stout's table has been modified to include the differences in density between tank water ρ_M and full-scale seawater ρ_S.

8.3. Test methods

Van Dyck (1989) discusses the various types of towing tests that are made on seaplane models.

Resistance and takeoff tests are accomplished with one of the following tests:

1) Specific test
2) NACA general test
3) Stevens collapsed data set

The Specific Test is when a model is built of a particular design and tested exactly according to the design displacement, center of gravity, and takeoff speed. This provides a direct prediction of full-scale performance; however, the results are not useful for future designs.

The NACA general test is an extensive characterization of the seaplane, requiring a large matrix of displacements and trim angles. From this, nondimensional coefficients for speed, draft, lift, resistance, and pitching moment are computed, allowing the results to be expanded to any size. To make performance predictions for a given design, points must be retrieved from a variety of plots and put together to develop a curve similar to the specific test.

In response to the difficulty of performing a complete NACA general test, researchers at Stevens Institute developed some approximate coefficients that were found to collapse the general test data well. As a result, they found that they could make less test runs to populate the matrix of conditions, provided the tests agreed with the assumptions. The primary assumptions in the Stevens Collapsed Data Set are that at lower speeds, the resistance coefficient is a function of the Volumetric Froude Number; whereas at high speeds, the resistance coefficient is a function of the lift coefficient. This assumption has been verified many times over for planing craft. Figure 25 showed a typical Stevens Collapsed Data Set. It won't be immediately clear to the reader that the combination of NACA coefficients $\frac{C_V^2}{C_\Delta^{\frac{1}{3}}}$ is related to the volume Froude number, but recognizing that $\nabla = \frac{\Delta}{\rho g}$ and collecting terms results in the following:

$$\frac{C_V^2}{C_\Delta^{\frac{1}{3}}} = \frac{\left(\frac{V}{\sqrt{gB}}\right)^2}{\left(\frac{\Delta}{\rho g B^3}\right)^{\frac{1}{3}}} = \frac{\frac{V^2}{gB}}{\frac{\nabla^{\frac{1}{3}}}{B}} = \frac{V^2}{g\nabla^{\frac{1}{3}}} = F_\nabla^2$$

Likewise, the combination of coefficients $\frac{\sqrt{C_\Delta}}{C_V}$ becomes $\sqrt{\frac{\Delta}{\rho g B^2}} = \sqrt{\frac{C_L}{2}}$.

9. Model tests of student design

Recently, a conceptual design was carried out by U.S. Naval Academy midshipmen Duncan Mamer, Joseph Esposito, Stuart Shrum, and Richard Stieger, as part of a 2-semester undergraduate design project, using many of the methods described in this article. The design was for a large amphibious cargo transport plane, with similar capacity to the C-130. This section discusses the development of the test apparatus and the principal findings of the test.

9.1. USNA seaplane Test apparatus

As part of the design project, we developed a seaplane test apparatus for the U.S. Naval Academy Hydromechanics Laboratory. The purpose of the apparatus was to enable the following types of testing:

1) Free-to-trim resistance testing
2) Fixed-trim high-speed resistance
3) Porpoising
4) Spray

The design closely followed the Davidson Laboratory seaplane test rig. Figure 32 shows a photograph of the test apparatus. Because the model has to be unloaded to zero weight for takeoff, it is best to maintain as light an apparatus as possible. This towing rig consisted of two aluminum rods running through linear bearings to permit freedom to heave. Heave was measured using a potentiometer with a pulley. The weights could be adjusted on the model using weight pegs with speed nuts (these can be made with aluminum 4-arm knobs drilled diagonally, so they drop over the threaded rod and lock in when tightened). It is important to be able to adjust weights quickly as they are moved often in seaplane tests. The lift due to the wings is represented by a mechanical lever unloader. This particular unloader used a 2:1 ratio to permit less mass of weights. The trim angle was measured using an inclinometer with reference to the horizon.

Fixed-trim tests were accomplished by attaching a bar (Fig. 33D) to the model. This bar is located below the drag gauge so that it does not impact the resistance measurements. There was a knob on the bar to permit trim adjustment, while reading the voltage from the inclinometer, to set the correct angle.

When testing for porpoising, it is necessary to include the effect of aerodynamic lift and damping on the horizontal

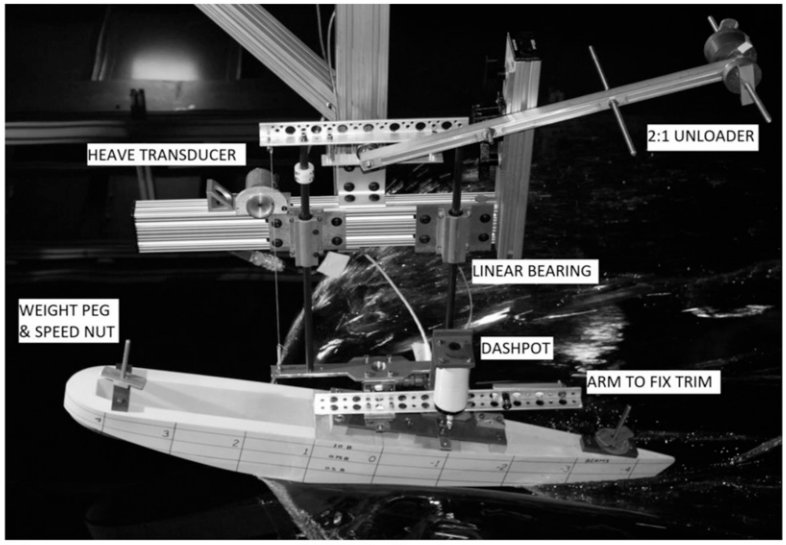

(A) USNA Seaplane Apparatus

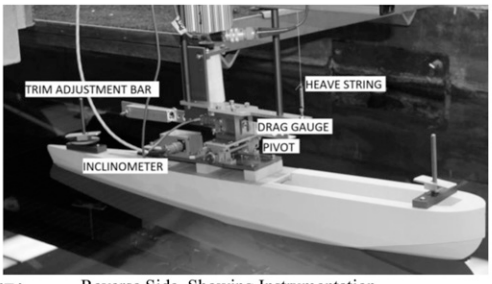

(B) Reverse Side, Showing Instrumentation

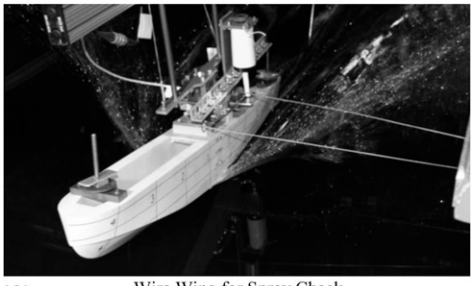

(C) Wire Wing for Spray Check

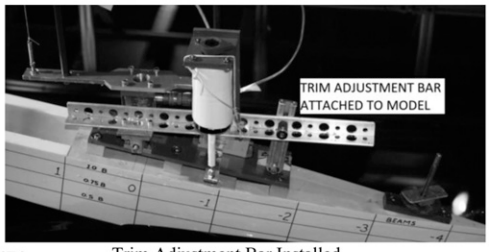

(D) Trim Adjustment Bar Installed

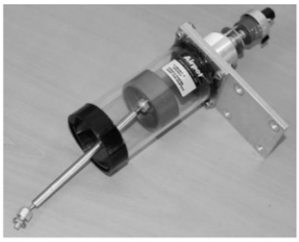

(E) Dashpot for Porpoising Tests

Fig. 32 USNA seaplane apparatus

elevators. Equation 1 of Locke (1943) shows how to compute the aerodynamic tail damping (which is pitch moment divided by pitch rate).

$$M_q = K\,\frac{\rho_a}{2} S_t l_t^2 V \left(\frac{dC_L}{d\alpha}\right)_t$$

where M_q is the aerodynamic pitch damping rate (moment/angular velocity), V is the speed, S_t is the surface area of the tail, l_t is the distance from the center of gravity to the tail, ρ_a is the density of air, $\left(\frac{dC_L}{d\alpha}\right)_t$ is the lift curve slope of the tail.

(K is a factor taken to be approximately 1.0.)

It will be seen that M_q varies with speed and length to the fourth power. In nondimensional format, suitable for model scaling:

$$\frac{M_q}{V\frac{\rho_w}{2}b^4} = \text{const}$$

This constant damping is on average .25 for many seaplanes.

In model testing, dashpots are used to provide this pitching moment. Dashpots often use oil, the weight of which is varied for different settings. The dashpot used in the present test (Fig. 33E) used air and was adjustable with a valve on the top of it. To calibrate the dashpot setting, the model was held out of the water and a weight was placed on the aft weight peg and the model released. The weight and distance provided the pitching moment, and the time history of the pitch motion provided the pitch velocity.

In addition to modeling damping, the pitch gyradius must also be accurate. Typical seaplanes (Locke 1943) have a pitch gyradius of .227 times the length of the seaplane—very close to the typical value of .25 used for ships.

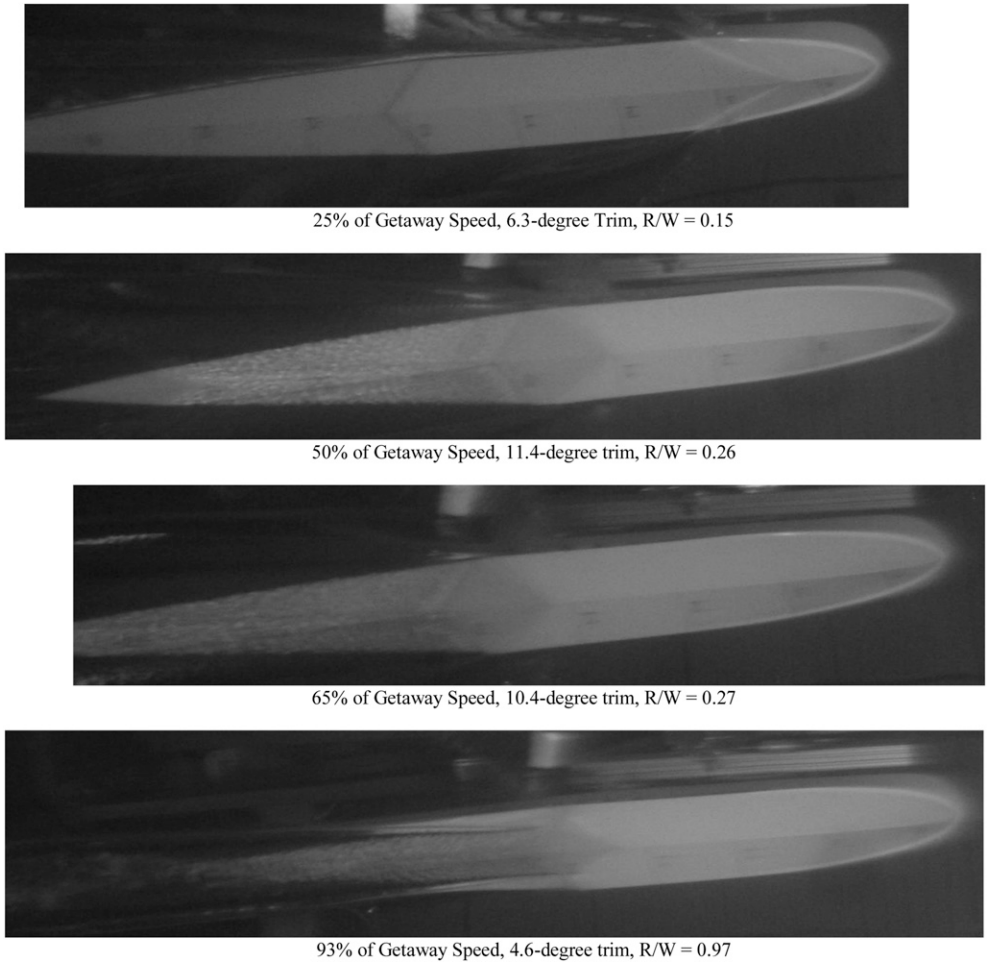

Fig. 33 Underwater photographs showing wetted area of the hull (note, camera is rotated and hull is going straight)

The effect of aerodynamic tail lift was computed by determining the additional pitching moment put on the seaplane as a function of change in the angle of attack. (This uses the lift curve slope, and the moment arm from the Longitudinal Center of Gravity (LCG) to the horizontal elevators.) This moment was represented by the addition of a flat spring (made of a piece of plastic), with holes drilled at regular intervals along its length, and a turnbuckle placed between the spring and the model. Spray tests were made by building a wire representation of the location of the wing (Fig. 33C) and observing whether the spray impacted the wing.

9.2. Underwater photographs

Underwater photography provides insights into the measurements during tests. Figure 33 shows underwater photographs of the tests at various speeds. The model had pitch instabilities, so the dashpot was used to damp them out to record static results.

The top photograph (25% of getaway speed) shows that the hull is mostly wetted and the step has not ventilated yet. This condition is similar to the hydrostatic condition.

As speed increases to 50% of the getaway speed, there is the characteristic ventilation aft of the step but reattachment near the tail of the aircraft. This speed also corresponds to the hump in the resistance curve, which for this design was at 40–50% of the getaway speed.

At 65% of the getaway speed, the model is running on the forebody alone, balancing on the small area forward of the step. At 93% the photograph shows the spray root crossing the step and the spray impinging on the afterbody. This condition can lead to large increases in resistance and dynamic instabilities. Whereas the resistance-to-weight ratio for this hull was generally around .25 for planing speeds, there was very little reduction in resistance as takeoff approached, and the load on the water became very small. As a result, the resistance-to-weight ratio before takeoff was approaching unity! This is a problematic speed for takeoff, where the induced drag of the wings is large and so is the hydrodynamic resistance. Drag due to spray wetting the afterbody is not easily predicted but can sometimes become a primary concern for whether there is enough thrust to take off.

9.3. Test findings

This design was developed by a group of undergraduate students with no prior training in seaplane design, using a variety of technical references written over an 80-year span. The model tests are a

Table 1 Dimensional conversions for Froude scaling of dynamically similar models (Adapted Stout 1950)

Unit	General conversion	$1/8^{th}$ scale ($\lambda = 8$)
Linear dimensions	λ^{-1}	1/8
Area	λ^{-2}	1/64
Volume	λ^{-3}	1/512
Mass, force	$\lambda^{-3}\,(\rho_M/\rho_S)$	~1/512
Moment	$\lambda^{-4}\,(\rho_M/\rho_S)$	~1/4096
Moment of inertia	$\lambda^{-5}\,(\rho_M/\rho_S)$	~1/32,768
Linear velocity	$\lambda^{-1/2}$	1/2.83
Linear acceleration	Constant	1
Angular velocity	$\lambda^{1/2}$	2.83
Angular acceleration	Λ	8
Time	$\lambda^{-1/2}$	1/2.83
R.P.M.	$\lambda^{1/2}$	2.83
Power	$\lambda^{-3.5}\,(\rho_M/\rho_S)$	~1/1448
Wing loading	$\lambda^{-1}\,(\rho_M/\rho_S)$	~1/8

valuable way to identify errors in the design, as well as identify factors that could not be predicted using the archival data. The principal findings of these particular tests were as follows:

1) The resistance values agreed well with the standard series that were used. This should not be a surprise as the hull was partially based on the geometry of the standard series.
2) The spray tests demonstrated that the spray would reach up toward the wings, which would cause erosion of the propellers. This observation contrasted their predictions using archival data from the standard series. After-the-fact analysis showed that this problem could have been predicted based on the K2 factor of the design, which was .024. According to Stout (1950), this design should have generated "excessive spray."
3) The initial hull design porpoised or skipped during both free-to-trim and fixed-trim tests at speeds above 80% of the takeoff speed. The porpoising was so violent that it was clear that the initial design was not feasible.

The hull design had included a pointed, faired step, similar to the "concave fairing" design shown earlier in this report. The step height was as recommended by Locke (1946).

The model was subsequently modified, removing the step fairing, so it looked like the "normal step" in the figure shown earlier. In addition, ventilation tubes were inserted just aft of the step to break any potential suction. The modification of the step improved the skipping performance markedly, but the hull was still unsatisfactory. Variations in the longitudinal center of gravity and loading were attempted. Ultimately, the students ran out of time during their test window to continue step modifications.

After-the-fact analysis showed that Locke's (1946) report was limited to length-to-beam ratios of 6, typical of WWII seaplanes, whereas the student design was closer to 10. Olson and Land (1948) had addressed this problem with a formula that included afterbody length. This is why earlier in this article, I recommend Olson and Land's criteria.

Although the results of the testing were unsatisfactory for the students, they revealed design problems that were not identified by the methods that the students had used, however carefully they were applied. The next design iteration of the design would include a larger step height and a reduced bottom loading to limit spray. A very simple rig, with a small model, can go a long way toward pointing out major problems before the design progresses too far.

10. Conclusions

This article has summarized some of the basics of seaplane design and hydrodynamic evaluation, based on recent experience in offering this topic in an educational setting. A model testing procedure is described, and it is shown how model tests can identify important design problems at early phases when they can still be corrected inexpensively.

Acknowledgments

This study is based in large part upon the Stevens Institute graduate course on Hydrodynamic Design of Seaplanes, which was originally taught by B.V. Korvin-Kroukovsky in the late 1940s and then by Daniel Savitsky in the mid-1950s. The author would like to recognize Dr. Daniel Savitsky for teaching this material to me during my time at Stevens Institute, enabling my further studies in this area. Midshipmen Duncan Mamer, Joseph Esposito, Stuart Shrum, and Richard Steiger developed the conceptual design and performed the model tests presented in this paper. John Zseleczky, USNA Hydromechanics Branch Head, provided use of the towing facilities. Mark Pavkov assisted in setting up and running the towing tests, and Donald Bunker assisted in the development of the towing apparatus.

References

Anon 2004 *Seaplane, Skiplane and Float/Ski Equipped Helicopter Operations Handbook*, U.S. Department of Transportation, Federal Aviation Administration, Flight Standards Service (https://www.faa.gov/regulations_policies/handbooks_manuals/aviation/seaplane_handbook/).

Bellanca, A. and Matthews, C. 2005 The Potential Effect of Maturing Technology upon Future Seaplanes, Report No. NAWCADPAX/TR.-2005/230, Patuxent River, MD: Naval Air Warfare Center Aircraft Division.

Batterson, S. A. and McArver, A. E. 1950 Water Landing Investigation of a Model Having a Heavy Beam Loading and a 30° Angle of Dead Rise, NACA Technical Note 2015.

Brizzolara, S., Judge, C., and Beaver, W. 2016 High deadrise stepped cambered planing hulls with hydrofoils: SCPH2. A proof of concept, *SNAME Transactions*, **124**, 312–321.

Carter, A. W. 1947 Comparison of Design Specifications with the Actual Static Transverse Stability of 25 Seaplanes, N.A.C.A. Technical Note No. 1253.

Celano, T. 1998 *Prediction of Porpoising Inception for Modern Planing Craft*, Transactions. Jersey City, NJ: Society of Naval Architects and Marine Engineers.

Clement, E. P. 1969 The Design of Cambered Planing Surfaces for Small Motorboats, Bethesda, MD: David Taylor Model Basin Report No. 3011.

Clement, E. P. and Hoyt, J. G. 2008 A parametric study of dynaplane-type planing motorboats, *Proceedings*, 1st Chesapeake Power Boat Symposium, March 7–8, Annapolis, MD.

Cooper, D. and Kennell, C. 2015 Summary of Historical Seaplane Data, Technical Report NSWCCD-CISD-2015/001, Bethesda, MD: Naval Architecture and Engineering Department.

Davidson, K. S. M. and Locke, F. W. S., Jr. 1943 *Some Analyses of Systematic Experiments on the Resistance and Porpoising Characteristics of Flying-Boat Hulls*, National Advisory Committee for Aeronautics, Wartime Report, Advance Restricted Report 3106.

Davidson, K. S. M. and Locke, F. W. S. 1944 General Tank Tests on the Hydrodynamic Characteristics of Four Flying Boat Hull Models of Differing Length-Beam Ratio, N.A.C.A. A.R.R. No. 4F15.

Dala, L. 2015 Dynamic stability of a seaplane in takeoff. *Journal of Aircraft*, **52**(3), 964–971.

DATHE, I. AND DE LEO, M. 1989 Hydrodynamic characteristics of seaplanes as affected by hull shape parameters, *Proceedings*, Intersociety Advanced Marine Vehicles Conference, June 5–7, Arlington, VA, 275–284.

DENZ, T., SMITH,S., AND SHRESTHA, R. 2007 Seaplane Economics: A Quantitative Cost Comparison of Seaplanes and Land Planes for Sea Base Operations, Total Ship Systems Directorate Technical Report NSWCCD-CISD-2007/07, Bethesda, MD: Naval Surface Warfare Center Carderock Division.

DECALLIES, R. N. 1958 *Hydrodynamics Manual*, Patuxent River, MD: Naval Air Test Center Flight Test Division.

DIEHL, W. S. 1924 Static Stability of Seaplane Floats and Hulls, N. A. C. A. Technical Note No. 183.

DIEHL. W. S. 1986 *Engineering Aerodynamics*. Revised Edition. Bethesda, MD: David W. Taylor Naval Ship Research and Development Center.

DU, H., FAN, G., AND YI, J. 2014 Autonomous takeoff control system design for unmanned seaplanes, *Ocean Engineering*, **85**, 21–31

DUAN, X. SUN, W., CHEN, C., WEI, M., AND YANG, Y. 2019 Numerical investigation of the porpoising motion of a seaplane planing on water with high speeds, *Aerospace Science and Technology*, **84**, 980–994

FENG, S., MINGZHEN, W, JIAXU, Z, AND QI, H 2020 Numerical simulation method for wave surface landing of seaplane, *IOP Conference Series Materials Science and Engineering*, **751**, 012061.

GOBBI, G., SMRCEK, L., GALBRAITH, R., LIGHTENING, B., STRÄTER, B., AND MAJKA, A, 2011 Report on current strength and weaknesses of existing seaplane/amphibian transport system as well as future opportunities. *FUSETRA. Report Prepared for European Union Directorate-General for Energy and Transport*.

HAAR, M. 1952 Effect of Forebody-Afterbody Proportions and Length-Beam Ratio on the Hydrodynamic Characteristics of a Series of Flying-Boat Hull Models. Experimental Towing Tank Report 465. Hoboken, NJ: Stevens Institute of Technology, Prepared for the Bureau of Aeronautics, Department of the Navy.

HAYHURST, K. J., NEOGI, N., AND VERSTYNEN, H. A. 2014 A Review of Current and Prospective Factors for Classification of Civil Unmanned Aircraft Systems. NASA/TM-2014-218511.

HUGLI, W. C. AND AXT, W. C. 1951 Hydrodynamic investigation of a series of hull models suitable for small flying boats and Amphibians, NACA Technical Note 2503.

HUGLI, W. C. AND VAN DYCK, R. L. 1955 A limitations analysis of hulls and hydro-skis for water-based aircraft, Experimental Towing Tank Technical Report No. 562, Hoboken, NJ: Stevens Institute of Technology. Prepared for U.S. Bureau of Aeronautics.

KORVIN-KROUKOVSKY, B. V. 1955 *Hydrodynamic Design of Seaplanes I*, Stevens Institute of Technology Course Notes, Hoboken, NJ: Davidson Laboratory.

KROO, I. AND SHEVELL, R. 2006 *Aircraft Design: Synthesis and Analysis" Version 1.2*, Stanford, CA: Desktop Aeronautics, Inc.

LOCKE, F. W. S. 1943 General Porpoising Tests of Flying-Boat-Hull Models, Advanced Restricted Report 3I17, Washington, DC: National Advisory Committee for Aeronautics.

LOCKE, F. W. S. 1944 General Resistance Tests on Flying-Boat Hull Models, National Advisory Committee for Aeronautics Advance Restricted Report 4B19.

LOCKE, F. W. S. 1946 An Analysis of the Skipping Characteristics of Some Full-Size Flying Boats, N.A.C.A. Wartime Report W-104.

LOCKE, F. W. S. 1947 A Collection of the Collapsed Results of General Tank Tests of Miscellaneous Flying-Boat-Hull Models, NACA Technical Note No. 1182.

LOCKE, F. W. S. 1953 The Effect of Size and Speed on Flying Boat Structural Weights, Report No. DR 1389, Washington, DC: Navy Department Bureau of Aeronautics.

LORIO, J., MORABITO, M. G. AND PAVKOV, M. E. 2015 Exploratory Towing Tests of Seaplane Skipping. *Proceedings*, 13th International Conference on Fast Sea Transportation, FAST, September 1–4, Washington, DC.

MAJKA, A. AND WAGNER, W. 2011 Requirements for a future seaplane/amphibian transport system. *FUSETRA*. Report Prepared for European Union Directorate-General for Energy and Transport.

MILWITZKY, B. 1948 A Generalized Theoretical and Experimental Investigation of the Motions and Hydrodynamic Loads Experienced by V-Bottom Seaplanes During Step-Landing Impacts. NACA Technical Note No. 1516.

MOHR, B. AND SCHOMANN, J. 2011 *Seaplane Data Base. FUSETRA*, Report Prepared for European Union Directorate-General for Energy and Transport.

NEBYLOV, V. AND NEBYLOV, A. 2011 Seaplane Landing Smart Control at Wave Disturbances. *Proceedings*, 18th IFAC World Congress, August 28–September 2, Milano, Italy.

ODEDRA, J., HOPE, G., AND KENNELL, C. 2004 *Use of Seaplanes and Integration within a Sea Base*, Total Ship Systems Directorate Technical Report NSWCCD-20-TR-2004/08, Bethesda, MD: Naval Surface Warfare Center Carderock Division.

OLSON, R. E. AND LAND, N. S. 1948 Effect of Afterbody Length and Keel Angle on Minimum Depth of Step for Landing Stability and on Take-Off Stability of a Flying Boat, N.A.C.A. Technical Note No. 1571.

PARKINSON, J. B. 1943 Design criterions for the dimensions of the forebody of a long-range flying boat. N.A.C.A. A.R.R. No. 3K08.

PARKINSON, J. B. 1948 Take-off performance of light twin-float seaplanes. National Advisory Committee for Aeronautics Technical Note No. 1524.

PARKINSON, J. B. 1955 NACA Model Investigations of Seaplanes in Waves. N. A. C. A. Technical Note 3419.

PEPPER, P. A. AND KAPLAN, L. 1966 Survey on Seaplane Hydro-Ski Design Technology – Phase 1: Qualitative Study, Prepared by Edo Corporation for the Office of Naval Research and the Naval Air Systems Command, Department of the Navy Report 7489-1.

PEPPER, P. A. AND KAPLAN, L. 1968 *Survey on Seaplane Hydro-Ski Design Technology – Phase 2: Quantitative Study*. Prepared by Edo Corporation for the Office of Naval Research and the Naval Air Systems Command. Department of the Navy Report 7489-2.

PIERSON, J. D. 1944 Directional stability of flying boat hulls during taxiing, *Journal of the Aeronautical Sciences*, **11**, 189.

QIU, L. AND SONG, W. 2016 Amphibious aircraft fuselage steps with decoupled hydrodynamic and aerodynamic analysis models, *Journal of Aerospace Engineering*, **29**(3), 10.1061/(ASCE)AS.1943-5525.0000557.

SAVITSKY, D. 1951 Wetted length and center of pressure of vee-step planing surfaces, Experimental Towing Tank Report 378, Prepared for the Office of Naval Research, Hoboken, NJ: Stevens Institute of Technology.

SAVITSKY, D. 1964 Hydrodynamic design of planing hulls. *Marine Technology*, **1**, 71–95.

SAVITSKY, D. 2012 The effect of bottom warp on the performance of planing hulls, Third Chesapeake Power Boat Symposium, June 15–16, Annapolis, MD.

SAVITSKY, D. AND BRESLIN, J. 1958 *On the Main Spray Generated by Planing Surfaces*, Hoboken, NJ: Davidson Laboratory Report, Stevens Instite of Technology.

SAVITSKY, D. AND MORABITO, M. G. 2011 Origin and characteristics of the main spray patterns generated by planing hulls. *Journal of Ship Production and Design* **27**, 63–83.

SMITH, A. G. AND ALLEN, J. E. 1954 *Water and Air Performance of Seaplane Hulls as Affected by Fairing and Fineness Ratio*. Aeronautical Research Council Reports and Memoranda No. 2896, United Kingdom.

STOUT, E. G. 1950 Development of high-speed water-based aircraft, *Journal of the Aeronautical Sciences*, **17**, 457–480.

STRUMPF, A. 1947 Model Tests on a Standard Series of Flying-Boat Hulls, Experimental Towing Tank Report No. 325, Hoboken, NJ: Stevens Institute of Technology.

SUYDAM, H. B. 1952 Hydrodynamic Characteristics of a Low-Drag Planing-Tail Flying-Boat Hull, Washington, DC: N.A.C.A. Technical Note 2481.

TOMASZEWSKI, K. M. 1946 Hydrodynamic Design of Seaplane Floats. Ministry of Supply. Aeronautical Research Council Current Papers. Royal Aircraft Establishment Report No. Aero 2154.

VAN DYCK, R. L. 1954 An Investigation of the Effect of Vee-Step Angle on the Hydrodynamic Characteristics of Seaplanes, Experimental Towing Tank Report 532, Prepared for the Bureau of Aeronautics, Department of the Navy, Hoboken, NJ: Stevens Institute of Technology.

VAN DYCK, R. L. 1958 *A Constant-Speed Method for Obtaining Rough Water Lanidng Impact Characteristics of Water-Based Aircraft*, Davidson Laboratory Report No 682, Hoboken, NJ: Stevens Institute of Technology. Prepared for Bureau of Aeronautics.

VAN DYCK, R. L. 1989 Seaplanes and the Towing Tank. Advanced Marine Vehicles Conference, June 5–7, Arlington, VA, 294–304.

VON KARMAN, T 1929 The Impact of Seaplane Floats during Landing. NACA Technical Note No. 321, Aachen, Germany: Aerodynamic Institute of the Technical High School.

WAGNER, H. 1931 Landing of Seaplanes, NACA Technical Memo No 622.

YING-GU, Z, GUO-LIANG, F, AND JIANQIANG, Y 2011 Modeling longitudinal aerodynamic and hydrodynamic effects of a flying boat in calm water, *Proceedings*, 2011 IEEE Internal Conference on Mechatronics and Automation, August 7–10, Beijing, China, 2039–2044.

XAO, Z., WU, B., WANG, M., AND HU, Q. 2019 Investigation of blocking effect of aviation high-speed towing tank based on CFD and EFD, *IOP Conference Series: Materials Science and Engineering*, Vol. **692**, *Proceedings*, 5th International Conference on Mechanical Engineering and Automation Science (ICMEAS 2019), October 10–12, Wuhan, China.